



Available online at www.sciencedirect.com



International Journal of Fatigue 00 (2017) 1–69

Journal
Logo

A new strategy for fatigue analysis in presence of general multiaxial time varying loadings

Ma Zepeng^{a,*}, Patrick Le Tallec^b, Habibou Maitournam^c

^a*Laboratory of Solid Mechanics, Ecole Polytechnique, 91128 Palaiseau Cedex, France*

^b*Laboratory of Solid Mechanics, Ecole Polytechnique, 91128 Palaiseau Cedex, France*

^c*IMSIA, ENSTA ParisTech, CNRS, CEA, EDF, Université Paris-Saclay, 828 bd des Maréchaux, 91762 Palaiseau cedex France*

Abstract

The object of this paper is to propose an energy based fatigue approach which handles multidimensional time varying loading histories.

Our fundamental thought is to assume that the energy dissipated at small scales governs fatigue at failure. The basis of our model is to consider a plastic behavior at the mesoscopic scale with a dependence of the yield function not only on the deviatoric part of the stress but also on the hydrostatic part. A kinematic hardening under the assumption of associative plasticity is also considered. We also follow the Dang Van paradigm at macro scale. The structure is elastic at the macroscopic scale. At each material points, there is a stochastic distribution of weak points which will undergo strong plastic yielding, which contribute to energy dissipation without affecting the overall macroscopic stress.

Instead of using the number of cycles, we use the concept of loading history. To accommodate real life loading history more accurately, mean stress effect is taken into account in mesoscopic yield function and non-linear damage accumulation law are also considered in our model. Fatigue will then be determined from the plastic shakedown cycle and from a phenomenological fatigue law linking lifetime and accumulated mesoscopic plastic dissipation.

Keywords: Fatigue; Energy; High cycle; Plasticity; Mean stress

*Corresponding author. Email address: zepeng.ma@polytechnique.edu

Nomenclature

S_{max}	maximum deviatoric stress during the loading cycles
σ_{-1}	fatigue limit for fully reversed condition
b	back stress
\dot{w}	energy dissipation rate at a certain scale
\dot{W}	energy dissipation rate at all scales
W	dissipated energy at all scales per unit time
W_{cyc}	dissipated energy at all scales per cycle
N	current number of cycles
N_F	number of cycles to failure
$\dot{\varepsilon}_p$	rate of effective plastic strain
W_0	reference density of damage energy
E	Young's modulus
$k = 500 \sim 800 \text{ MPa}$	hardening parameter
$\beta = 1 \sim 50$	weakening scales distribution exponent
$\gamma = 0 \sim 50$	material parameter from Chaboche law
$\alpha = 1 - a \left(\frac{\frac{1}{2}J_2(t) - \sigma_{-1} (1 - 3c\sigma_{H,max}(t))}{\sigma_u - J_2(t)} \right)$	characterizes non-linearity of damage accumulation(c is constant)
J_2	The second principal invariant of the stress deviatoric tensor
a	material parameter from Chaboche law
M_0	material parameter in Chaboche law
σ_y	macroscopic yield stress(normal or shear)
$\lambda = 0 \sim 5$	hydrostatic pressure sensitivity
$\underline{\underline{S}} = \text{dev} \dot{\underline{\underline{\Sigma}}}$	deviatoric part of the stress tensor
Σ_H	macroscopic hydrostatic pressure
$A_{II} = \tau_{oct,a} = \sqrt{\frac{1}{6}J_2}$	the amplitude of octahedral shear stress
$\sigma_{VM} = \sqrt{3J_2}$	Von Mises stress
s_{-1}	tensile fatigue limit for $R = -1$
$\langle \rangle$	Macaulay bracket symbol. $\langle \rangle$ is defined as $\langle m \rangle = 0$ if $m \leq 0$

1 Weakening scales and yield function

1.1. The concept of weakening scales

We follow the Dang Van paradigm. The structure is elastic at the macroscopic scale. At each material points, there is a stochastic distribution of weak points which will undergo strong plastic yielding, without contributing to the overall macroscopic stress. From a microscopic point of view, there is a distribution of weakening scales, namely $s \in [1, \infty)$. Let S_{max} be the macroscopic stress intensity at present time. Let σ_y be the yield limit before weakening. Then we imagine that for a given scale s :

- either $1 \leq s \leq \sigma_y/S_{max}$, then $S_{max} \leq \sigma_y/s$, the material stays in the elastic regime and there is no energy dissipation at this scale.
- or $\sigma_y/S_{max} \leq s \leq \infty$, then $S_{max} \geq \sigma_y/s$, the material is in the plastic regime and there is dissipated energy at scale s , contributing to the fatigue limit, which evolve through kinematic hardening.

In more details, at each scale s of a plastic evolution process there is a weakened yield limit σ_y/s , zero initial plastic strain $\underline{\underline{\varepsilon}}_p$ and zero initial backstress $\underline{\underline{b}}$ at initial time t_0 .

1.2. Distribution of weakening scales

We assume the weakening scales have a probability distribution function of power law:

$$P(s) = Hs^{-\beta},$$

where β is a material constant and H is hardening constant. The choice of a power law has two reasons: on one hand, this type of distribution corresponds to a scale invariant process, on the other hand it leads in cyclic loading to a prediction of a number of cycles to life limit as a power law function of the stress intensity. More general laws can also be proposed.

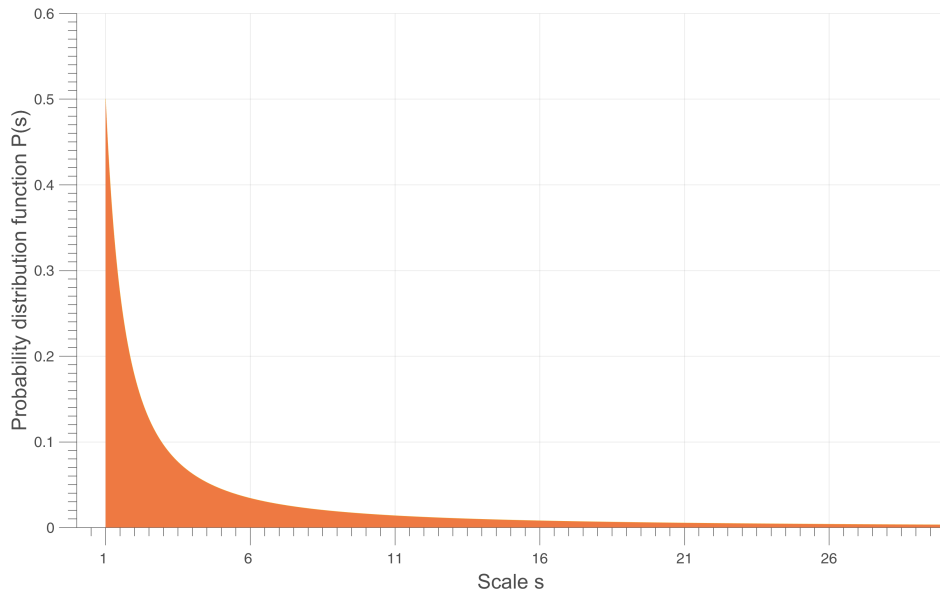
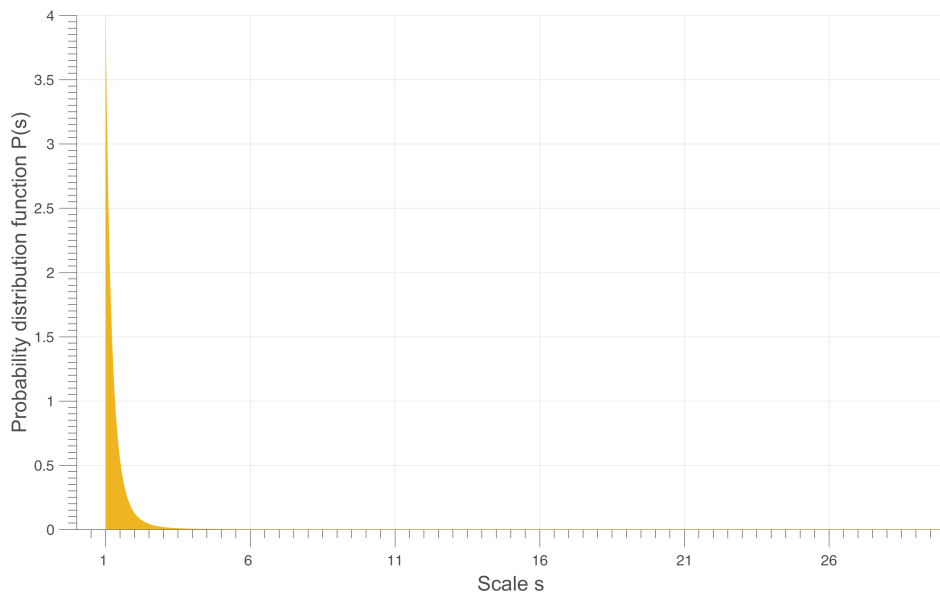
The integrated probability ranging from macroscopic to microscopic stress is unity. From this we can conclude:

$$\int_1^\infty P(s)ds = \left[\frac{Hs^{1-\beta}}{1-\beta} \right]_1^\infty = 0 - \frac{H}{1-\beta} = 1.$$

Then we know $H = \beta - 1$, so the distribution is given by:

$$P(s) = Hs^{-\beta} = (\beta - 1)s^{-\beta}$$

The probability of weakening scales is shown in Figure 1 and Figure 2. We can see smaller β has larger probability of weakening.

Figure 1: Weakening scales s probability distribution curve when $\beta = 1.5$ Figure 2: Weakening scales s probability distribution curve when $\beta = 5$

1.3. Yield function with mean stress effect

Positive mean stress clearly reduces the fatigue life of the material. In design evaluation of multiaxial fatigue with mean stress, a simplified, conservative relation between mean stress and equivalent alternating stress is necessary. We can improve the model by modifying the yield function σ_y and the localization tensor.

The idea is to consider as in Maitournam and Krebs[1] that the yield limit σ_y can be reduced in presence of positive mean stress. The mesoscopic yield function can therefore be written as:

$$f(s) = \|\underline{\underline{S}}(s) - \underline{\underline{b}}(s)\| + (\lambda \Sigma_H - \sigma_y) / s \leq 0 \quad (1)$$

with $\underline{\underline{S}}$ denoting the deviatoric part of the stress tensor at microscale, and $\underline{\underline{b}}(s)$ the corresponding backstress at the same scale. The material remain in elastic regime when $f < 0$ and in plastic regime when $f = 0$.

1.4. Local plastic model

First we should describe the mesoscopic stress state. The model considers a plastic behavior at the mesoscopic scale. The mesoscopic stress evolution equations are thus:

$$\dot{\underline{\underline{S}}}(s, M, t) = \text{dev} \dot{\underline{\underline{\Sigma}}}(M, t) - \frac{E}{1 + \nu} \dot{\underline{\underline{\varepsilon}}}^p(s, M, t), \quad (2)$$

which defines a Taylor-Lin scale transition model with unit localization tensor[2].

$$\dot{\underline{\underline{b}}}(s, M, t) = \frac{kE}{E - k} \dot{\underline{\underline{\varepsilon}}}^p(s, M, t), \quad (3)$$

which is our kinematic hardening model.

$$\dot{\underline{\underline{\varepsilon}}}^p(s, M, t) = C \frac{\partial f(s, M, t)}{\partial \underline{\underline{S}}}, \quad (4)$$

which is the associated plastic flow rule assuming $C = 0$ when $f < 0$ and $C \geq 0$ when $f = 0$.

Here E denotes the Young's modulus and k the hardening parameter. The local dissipated energy rate per volume at weakening scales s is given by the local entropy dissipation:

$$\dot{w}(s, M, t) = (\underline{\underline{S}} - \underline{\underline{b}})(s, M, t) : \dot{\underline{\underline{\varepsilon}}}^p(s, M, t). \quad (5)$$

2 Construction of an energy based fatigue approach

In a preliminary step, we will consider a simple macroscopic loading history $\underline{\underline{\Sigma}}(M, t)$ which is uniaxial and time periodic of deviatoric amplitude S_{max} , and a Von Mises flow rule to see if we get a prediction of local failure for a number of cycles N_F varying as $\Sigma^{-\beta}$.

In uniaxial cyclic loading, there will be 3 kinds of loading patterns, as is shown in Figure 3:

1. Elastic regime, in phase 2 and 4, where $\dot{\underline{\underline{\varepsilon}}}^p(s, M, t) = 0$, and $|\underline{\underline{S}} - \underline{\underline{b}}| < (\sigma_y - \lambda \Sigma_H) / s$.
2. Plastic regime according to plastic flow rule, with increasing plastic deformation, in phase 5 and 1, where $\dot{\underline{\underline{\varepsilon}}}^p(s, M, t) = C \frac{\underline{\underline{S}}(s) - \underline{\underline{b}}(s)}{\|\underline{\underline{S}}(s) - \underline{\underline{b}}(s)\|} > 0$ with $C = \text{dev} \dot{\underline{\underline{\Sigma}}} \left(\frac{kE}{E - k} + \frac{E}{1 + \nu} \right)^{-1}$, with $\underline{\underline{S}} - \underline{\underline{b}} = (\sigma_y - \lambda \Sigma_H) / s$ and $\dot{\underline{\underline{S}}} - \dot{\underline{\underline{b}}} = 0$.

3. Plastic regime in the other direction, in phase 3, there is $\dot{\varepsilon}^p(s, M, t) < 0$, then $\underline{S} - \underline{b} = -(\sigma_y - \lambda \Sigma_H) / s$ and $\dot{\underline{S}} - \dot{\underline{b}} = 0$

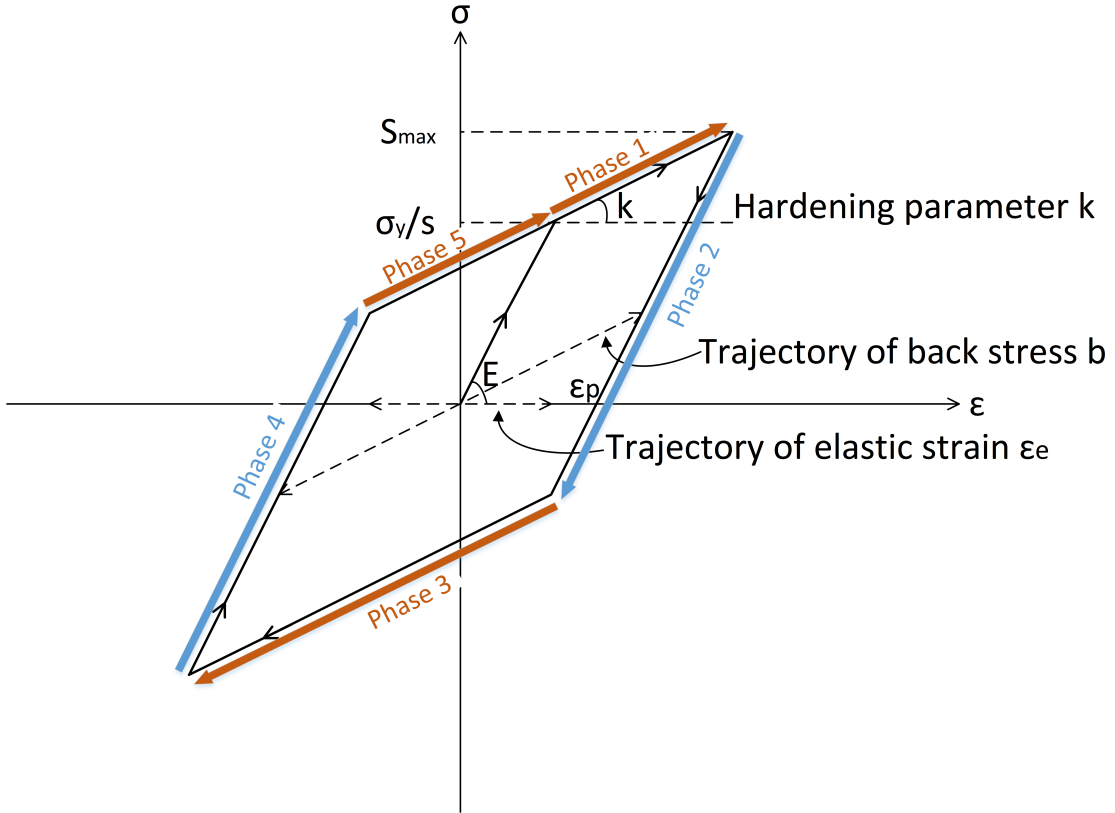


Figure 3: Uniaxial load with plastic dissipation

In phase 1, a direct analysis yields the energy dissipation at scale s :

$$dW = (S - b)d\varepsilon^p = \frac{(E - k)(1 + \nu)}{E(E + k\nu)} \frac{(\sigma_y - \lambda \Sigma_H)}{s} \left(S_{max} - \frac{(\sigma_y - \lambda \Sigma_H)}{s} \right) \quad (6)$$

A similar analysis yields

$$dW(\text{phase1}) = dW(\text{phase5}) = \frac{1}{2}dW(\text{phase3}).$$

We can then calculate the local dissipated energy W at point M during one cycle by cumulating the input of all sub-scales which result in plastic regime with their probabilities [3].

$$\begin{aligned} W_{cyc} &= 4 \int_{(\sigma_y - \lambda \Sigma_H)/S_{max}}^{\infty} dW(s, M, t)P(s)ds \\ &= 4 \int_{(\sigma_y - \lambda \Sigma_H)/S_{max}}^{\infty} \frac{(E - k)(1 + \nu)}{E(E + k\nu)} \frac{(\sigma_y - \lambda \Sigma_H)}{s} \left(S_{max} - \frac{(\sigma_y - \lambda \Sigma_H)}{s} \right) (\beta - 1) s^{-\beta} ds \\ &= \frac{4(E - k)(1 + \nu)(\beta - 1)}{E(E + k\nu)\beta(\beta + 1)} \frac{S_{max}^{\beta + 1}}{(\sigma_y - \lambda \Sigma_H)^{\beta - 1}}. \end{aligned} \quad (7)$$

So we have a power law relationship between stress intensity and the dissipated energy per cycle as Eq.(8).

$$W_{cyc} = C_1 S_{max}^{\beta+1}, \quad (8)$$

with

$$C_1 = f(\lambda, \beta) = \frac{4(E - k)(1 + \nu)(\beta - 1)}{E(E + k\nu)\beta(\beta + 1)(\sigma_y - \lambda\Sigma_H)^{\beta-1}}.$$

If the dissipated energy accumulates linearly until a failure value W_0 , we can get directly the number of cycles to failure from Eq.(9):

$$N_F = \frac{W_0}{W_{cyc}} = \frac{W_0}{C_1} S_{max}^{-\beta-1}. \quad (9)$$

As for the time to failure in cyclic loading, there is:

$$T_F = N_F t_{cyc}.$$

From Eq.(7), we then obtain that the model predicts as expected a power law dependence in function of S_{max} . However, experiments shows that the damage or the energy accumulation of a material evolves non-linearly in time. We should introduce below a method to handle such a nonlinearity.

3 Nonlinearity of damage accumulation

3.1. Energy approach with Chaboche law

The Chaboche law[4] is essentially a damage incremental law for cyclic loading of stress intensity σ with a deviatoric part A_{II} and hydrostatic part Σ_H , defining the damage increase by:

$$\delta D = \left(1 - (1 - D)^{\gamma+1}\right)^\alpha \left(\frac{A_{II}}{M(\sigma_H)(1 - D)}\right)^\gamma \delta N \quad (10)$$

With $A_{II}^* = A_{II} / (1 - D)$ evolving with damage D . And the mean stress effect is in both exponential α and denominator $M(\sigma_H)$.

$$\alpha = 1 - a \left(\frac{\frac{1}{2}J_2(t) - \sigma_{-1}M(\sigma_H)}{\sigma_u - J_2(t)} \right),$$

$$M(\sigma_H) = M_0 (1 - 3c\sigma_{H,max}(t)).$$

Eq.(10) writes equivalently as Eq.(11):

$$\delta[1 - (1 - D)^{\gamma+1}]^{1-\alpha} = (1 - \alpha)(\gamma + 1) \left(\frac{A_{II}}{M(\Sigma_H)}\right)^\gamma \delta N = \frac{1}{N_F(\sigma)} \delta N. \quad (11)$$

Here $N_F(\sigma)$ denotes the number of cycles at intensity σ to failure as obtained by integration of Eq.(11) from $D = 0$ to $D = 1$. In our model, in case of a simple uniaxial cyclic loading, we propose to replace $\frac{1}{N_F(\Sigma)}$ which is the relative unit increment of energy by $\frac{W_{cyc}(\Sigma)}{W_0}$.

The nonlinear damage incremental law using energy dissipation:

$$\begin{aligned}
 \delta D &= \frac{(1 - (1 - D)^{\gamma+1})^\alpha}{(1 - D)^\gamma} \delta W \\
 &= \frac{(1 - (1 - D)^{\gamma+1})^\alpha}{(1 - D)^\gamma} \frac{W_{cyc} \delta N}{W_0} \\
 &= \frac{(1 - (1 - D)^{\gamma+1})^\alpha}{(1 - D)^\gamma} \frac{4(E - k)(1 + \nu)(\beta - 1)}{E(E + k\nu)\beta(\beta + 1)} \frac{S_{max}^{\beta+1}}{(\sigma_y - \lambda\Sigma_H)^{\beta-1}} \frac{\delta N}{W_0}.
 \end{aligned} \tag{12}$$

We compare Eq.(10) and Eq.(12), in Chaboche model there is:

$$\beta + 1 = \gamma.$$

Similar to Eq.(11), we define here the “equivalent damage” \tilde{D} in Eq.(13):

$$\tilde{D} = 1 - (1 - D)^{\gamma+1}, \tag{13}$$

with D the damage variable introduced by Chaboche in its model to scale the stress intensity:

$$A_{II} \longrightarrow \frac{A_{II}}{1 - D}.$$

We have

- $\tilde{D} = 0$ when $D = 0$ (undamaged material),
- $\tilde{D} = 1$ when $D = 1$ (failure of material),

and a nonlinear relation in between as in Figure 4:

$$\delta\tilde{D} = (\gamma + 1)(1 - D)^\gamma \delta D.$$

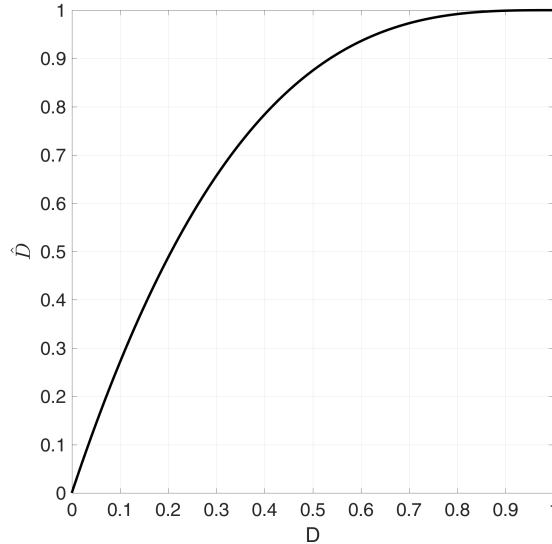
Change of damage measure $\tilde{D} = 1 - (1 - D)^{\gamma+1}$ makes the law explicit. The differential equation $\frac{d\tilde{D}}{dN} = c_D \tilde{D}^\alpha J_2^\gamma$ predicts a number of cycles to fatigue at constant load is given by

$$N_F = c_N \frac{1}{1 - \alpha} J_2^\gamma.$$

This method requires cycle counting which is difficult and technical for complex load histories. In addition, it has limited influence of multiaxiality.

Now in our model we use the same growth rule as in Chaboche in cyclic load regime, but replace stress intensity by multiscale dissipated energy (no cycle counting) in Eq.(14).

$$\frac{d\tilde{D}}{dN} = c_D \tilde{D}^\alpha J_2^\gamma \rightarrow \frac{d\tilde{D}}{dt} = \tilde{D}^\alpha \dot{W}/W_0.$$

Figure 4: The relation between \tilde{D} and D when $\gamma = 2$

$$\delta\tilde{D} = \tilde{D}^\alpha \frac{\delta W}{W_0} = \tilde{D}^\alpha \frac{W_{cyc} \delta N}{W_0}. \quad (14)$$

The number of cycles to failure in constant loading case, obtained by integrating D from 0 to 1 is:

$$N_F = \frac{W_0}{(1-\alpha) W_{cyc}} = \frac{W_0}{(1-\alpha) C_1} S_{max}^{-\beta-1}. \quad (15)$$

From Eq.(15), we see $(-\beta - 1)$ is related to the slope in S-N curve and $\frac{W_0}{C_1}$ defines the number of cycles to failure.

3.2. Generalized damage accumulation

Eq.(11) is a general accumulation law which can be applied for any cyclic loading sequence provided that we can identify the multiscale value of the dissipated energy per cycle.

But the notion of cycle itself may be hard to identify for general loadings. The idea is then to replace the relative increment of dissipated energy per cycle by the relative increment of dissipated energy per unit time, yielding Eq.(16):

$$\delta\tilde{D} = \tilde{D}^\alpha \frac{W}{W_0} = \tilde{D}^\alpha \frac{\dot{W} \delta t}{W_0} \quad (16)$$

giving equivalent differential form of damage accumulation:

$$\delta\tilde{D} = \tilde{D}^\alpha \frac{\dot{W} \delta t}{W_0} \quad (17)$$

The time to failure, obtained by integrating \tilde{D} from 0 to 1 is:

$$T_F = \frac{1}{1-\alpha} \frac{W_0}{\dot{W}}. \quad (18)$$

In differential form, the relation (19) writes from Eq.(16) and Eq.(18):

$$\delta \tilde{D}^{1-\alpha} = \frac{\delta t}{T_F}. \quad (19)$$

When we integrate Eq.(16) from 0 to \tilde{D} at constant loading conditions. The damage, expressed as a function of t/T_F is:

$$\tilde{D} = \left(\frac{t}{T_F} \right)^{\frac{1}{1-\alpha}}. \quad (20)$$

This expression is in good agreement with experimental results[4].

In a general loading case, \dot{W} is the microscopic energy dissipation rate of unit defect and W_0 is the energy threshold of unit defect. By integrating Eq.(5) over all microscales, we get:

$$\dot{W}(M, t) = \int_{s=1}^{\infty} \dot{w}(s, M, t) P(s) ds = \int_{s=1}^{\infty} (\underline{S} - \underline{b})(s, M, t) : \underline{\dot{\epsilon}}^p(s, M, t) P(s) ds. \quad (21)$$

The evolution of \underline{S} , \underline{b} and $\underline{\dot{\epsilon}}^p$ are given previously. Eq.(16) and (21) are therefore our proposed damage incremental law with energy dissipation.

This is a nonlinear law with a constant α , there will be no sequence effect. In other words, when applying two successive cycles of different intensities, the failure will occur at the same number of cycles whatever the order of the loading(high then low versus low then high). In numerical implementation of complex loading case, to take into account the load sequence effect, α changes at every time step.

We introduce s_{min} , which is the minimum scale that causes energy loss:

$$s_{min} = \frac{(\sigma_y - \lambda \Sigma_H)}{S_{max}}. \quad (22)$$

To take into account the sequence effect, the parameter α should change with S_{max} in order to handle change of cycle intensity and the influence on fatigue life.

3.3. Sequence effect

Experiments show fatigue tests started with high stress then change to low stress has less fatigue life than the combination of high stress life proportion plus the low one. This phenomenon of sequence effect is load history dependent, so we need a stress induced parameter to describe it.

This is done in Chaboche with three ingredients:

1. Notion of damage sensitive effective stress:

$$\sigma_D^{eff} = J_2(\underline{\Sigma}) / (1 - D)$$

2. $(\sigma_D^{eff})^\gamma$ controlled law for damage growth

$$\frac{dD}{dN} = c_\gamma \tilde{D}^\alpha (\sigma_D^{eff})^\gamma.$$

3. Load dependence of exponent α (from 1 at zero load to 0 at large loads).

Many fatigue damage accumulation models are based on the two level loading experiments which is one of the basic random loading analysis. To facilitate our verification of the law we use two-stress level loading, the specimen is firstly loaded at stress Σ_1 for T_1 cycles and then at stress Σ_2 for T_2 cycles until failure. We can then observe if the experimental results are satisfactory.

In Chaboche model, the proposition of α is:

$$\alpha = 1 - a \left(\frac{\sigma_{eq} - \sigma_{fatigue}}{\sigma_u - \sigma_{eq}} \right). \quad (23)$$

We propose a load dependent α through s_{min} (= the smallest scale experiencing plastic dissipation). Possible choice of α is expressed as Eq.(24):

$$\alpha = 1 - a \left(\frac{\frac{1}{s_{min}}}{1 - \frac{1}{s_{min}}} \right). \quad (24)$$

There is no notion of fatigue limit in our model, $\sigma_{fatigue} = 0$. The intensity of loading

$$\frac{\sigma_{eq} - \sigma_{fatigue}}{\sigma_u - \sigma_{eq}} = \frac{1}{\frac{\sigma_u}{\sigma_{eq}} - 1}$$

is measured by

$$\left(\frac{\frac{1}{s_{min}}}{1 - \frac{1}{s_{min}}} \right) = (s_{min} - 1)^{-1}.$$

This means that we measure the distance of load to ultimate failure by local variable s_{min} through

$$\frac{\sigma_u}{\sigma_{eq}} - 1 \longrightarrow (s_{min} - 1)$$

We have T_F expressed in Eq.(18) and differential form of damage accumulation in Eq.(17). Now we are able to chain two cycles $i = 1$ and $i = 2$ (at rate \dot{W}_i associated to exponent α_i). Firstly after loading time T_1 , we cycle from $\tilde{D} = 0$ to $\tilde{D} = \tilde{D}_1$ by integrating Eq.(19):

$$(1 - \tilde{D}_1)^{1-\alpha_1} = \frac{T_1}{T_{F1}} \quad (25)$$

then we cycle from $\tilde{D} = \tilde{D}_1$ to failure $\tilde{D} = 1$:

$$1 - (1 - \tilde{D}_1)^{1-\alpha_2} = \frac{T_2}{T_{F2}} \quad (26)$$

From Eq.(25) and Eq.(26), after elimination of $(1 - D_1)$ we get:

$$\frac{T_2}{T_{F2}} = 1 - \left(\frac{T_1}{T_{F1}} \right)^\eta, \quad (27)$$

with

$$\eta = \frac{1 - \alpha_2}{1 - \alpha_1}. \quad (28)$$

In the case of high-low loading sequence there is $\Sigma_1 > \Sigma_2$, meaning $S_{max1} > S_{max2}$, which gives $\alpha_1 < \alpha_2$, so we have:

$$\eta = \frac{1 - \alpha_2}{1 - \alpha_1} < 1 \implies \frac{T_2}{T_{F2}} = 1 - \left(\frac{T_1}{T_{F1}} \right)^\eta < 1 - \frac{T_1}{T_{F1}} \implies \frac{T_1}{T_{F1}} + \frac{T_2}{T_{F2}} < 1.$$

We can see from Figure 5 that cycling 1 for fifty percent of its failure time leaves a reserve before failure to cycle 2 much less than fifty percent. To conclude, the cumulative damage under high-low loading sequence, as we deduced, has the addition of partial lives less than unit. Similarly, the cumulative damage under low-high loading sequence has addition of partial lives more than 1.

$$\frac{T_1}{T_{F1}} + \frac{T_2}{T_{F2}} > 1$$

The curve is depicted in Figure 5. For constant two-level stress loading, $\alpha_1 = \alpha_2$, the Chaboche law returns to the Miner rule where:

$$\frac{T_1}{T_{F1}} + \frac{T_2}{T_{F2}} = 1$$

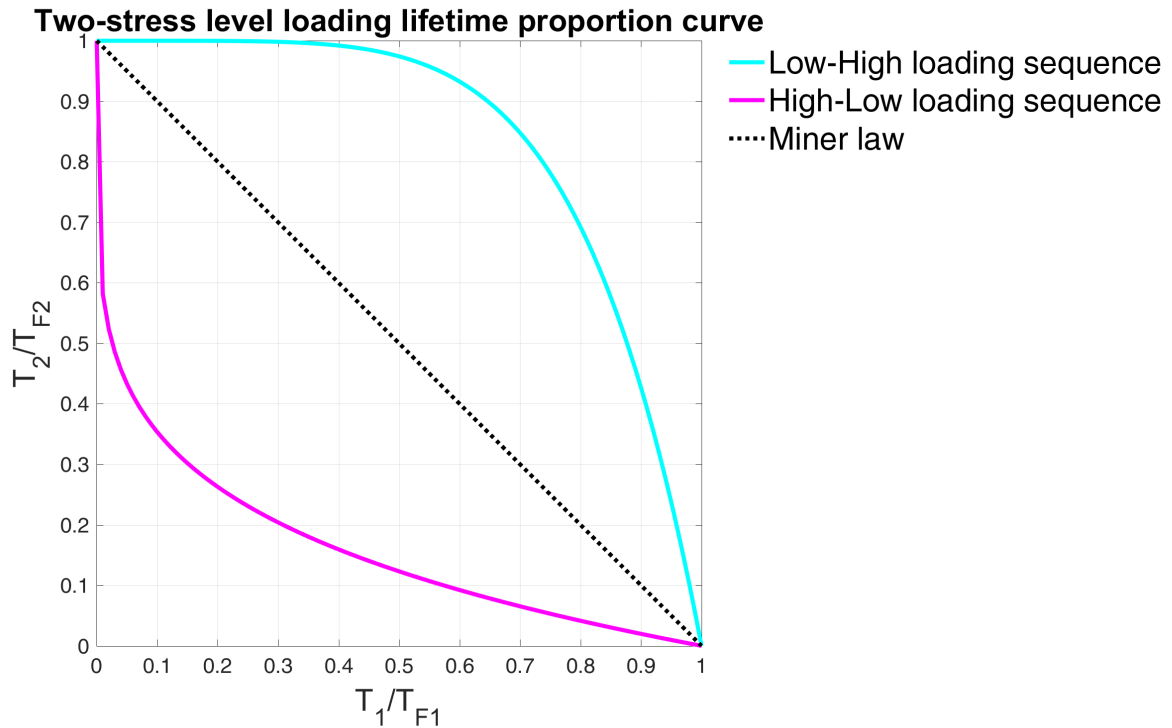


Figure 5: High to low and low to high loading sequence comparison

4 Numerical strategy

4.1. Integration rules for \dot{W} and $\delta\tilde{D}$

Our first approach takes one cycle as unit time. We compute analytically the energy dissipation at each scale during this cycle. The method is valid for simple loading history and which includes the integration on all weakening scales. The damage \tilde{D} is accumulated after each cycle.

However, there are certain limitations of this method. Firstly we need a load history decomposition in cycles. Secondly in real life the perfect close loop cycle is hardly applicable.

Thus we propose in Eq.(16) a more general method which can be integrated by a step by step strategy. We compute numerically the dissipation at different scales using an implicit Euler time integration of the

constitutive laws of section 1.4. After which we make a numerical integration on different scales. Then we can update the damage and go to next time step.

Instead of doing the scale integration directly which can be difficult for complex loading, the Gaussian Quadrature rule with Legendre points is used to give the value of local dissipated energy rate.

To use the Gaussian quadrature rule the limit range of integral must be from -1 to 1 , while the total dissipated energy is expressed by integrating all the weakening scale s ranging from 1 to infinity with their occurrence probabilities:

$$\dot{W} = \int_1^\infty \dot{w}(s)(\beta - 1)(s)^{-\beta} ds.$$

To change the limit range of integral from $[1, \infty]$ to $[1, 0]$ we take as new integration variable $u(s) = s^{-p}$ with $p = \beta - 1$, yielding $u(1) = 1$ and $u(\infty) = 0$ with

$$du = -ps^{-p-1} ds$$

that is

$$du = (-\beta + 1)s^{-\beta} ds = (-\beta + 1)u^{\frac{1}{1-\beta}} du.$$

Therefore the dissipated energy summed on all scales is:

$$\begin{aligned} \dot{W} &= \int_1^\infty \dot{w}(s)(\beta - 1)(s)^{-\beta} ds \\ &= \int_1^0 \dot{w}(u^{\frac{1}{1-\beta}})(\beta - 1) \frac{1}{-\beta + 1} du \\ &= \int_0^1 \dot{w}(u^{\frac{1}{1-\beta}})(\beta - 1) \frac{1}{\beta - 1} du \\ &= \int_0^1 \dot{w}(u^{\frac{1}{1-\beta}}) du \\ &= \frac{1}{2} \int_{-1}^1 \dot{w}\left[\left(\frac{x+1}{2}\right)^{\frac{1}{1-\beta}}\right] dx \end{aligned} \quad (29)$$

given $u = \frac{x+1}{2}$.

So the dissipated energy rate integrated over all scales takes the form of Eq.(30):

$$\dot{W} = \frac{1}{2} \int_{-1}^1 \dot{w}\left[\left(\frac{x+1}{2}\right)^{\frac{1}{1-\beta}}, t\right] dx \approx \frac{1}{2} \sum_i \omega_i \dot{w}\left[\left(\frac{x_i+1}{2}\right)^{\frac{1}{1-\beta}}, t\right], \quad (30)$$

where ω_i and x_i are respectively the weights and nodes of the Gauss Legendre integration rule used for the numerical integration. The use of Gaussian Quadrature rule changes the integrand s from infinity to finite fixed values without affecting the integration results. In this work, we used 64 points[5].

After changing the integration limit, $\left(\frac{x+1}{2}\right)^{\frac{1}{1-\beta}}$ represents the weakening scale s .

Damage accumulation is deduced from Eq.(16):

$$\tilde{D}_{n+1} = \tilde{D}_n + \tilde{D}_n^\alpha \frac{W}{W_0} \quad (31)$$

with $W = \dot{W}dt$ We upgrade the damage step by step following Eq.(31). When \tilde{D} reaches one, the material fails.

4.2. Regime determination under multiple scales

The material could be both in elastic and plastic regime at different scales. To be more elaborate, we reuse the fundamental equations in different regimes. At scale s , we have a dissipation rate given by:

$$\dot{w}(s) = \left(\underline{\underline{S}} - \underline{\underline{b}} \right) : \dot{\underline{\underline{\varepsilon}}}^p,$$

which differs between plastic and elastic regime.

Elastic regime:

There we have plastic strain rate $\dot{\underline{\underline{\varepsilon}}}^p = 0$, back stress rate $\dot{\underline{\underline{b}}} = 0$ and deviatoric stress rate $\dot{\underline{\underline{S}}} = \text{dev} \dot{\underline{\underline{\Sigma}}}$, leading to

$$\dot{\underline{\underline{S}}} - \dot{\underline{\underline{b}}} = \text{dev} \dot{\underline{\underline{\Sigma}}},$$

meaning

$$\left(\underline{\underline{S}} - \underline{\underline{b}} \right) (t + dt) = \left(\underline{\underline{S}} - \underline{\underline{b}} \right) (t) + \text{dev} \dot{\underline{\underline{\Sigma}}} dt.$$

At each time step we define a trial stress:

$$\left(\underline{\underline{S}} - \underline{\underline{b}} \right) (t + dt) := \left(\underline{\underline{S}} - \underline{\underline{b}} \right)_{\text{trial}}. \quad (32)$$

We are in elastic regime at scale s as long as we satisfy

$$\left(\underline{\underline{S}} - \underline{\underline{b}} \right)_{\text{trial}} \leq (\sigma_y - \lambda \Sigma_H) / s$$

Plastic regime:

When we leave elastic regime at scale s , we have:

$$\left\{ \begin{array}{ll} \dot{\underline{\underline{\varepsilon}}}^p = C \frac{\underline{\underline{S}} - \underline{\underline{b}}}{\| \underline{\underline{S}} - \underline{\underline{b}} \|}, C > 0, & \text{plastic flow,} \\ \| \underline{\underline{S}} - \underline{\underline{b}} \| = (\sigma_y - \lambda \Sigma_H) / s, & \text{yield limit,} \\ \left(\underline{\underline{S}} - \underline{\underline{b}} \right) : \left(\dot{\underline{\underline{S}}} - \dot{\underline{\underline{b}}} \right) = 0, & \text{yield limit time invariance,} \\ \dot{\underline{\underline{b}}} = \frac{kE}{E - k\underline{\underline{\varepsilon}}} \dot{\underline{\underline{\varepsilon}}}^p, & \text{kinematic hardening rule,} \\ \dot{\underline{\underline{S}}} = \text{dev} \dot{\underline{\underline{\Sigma}}} - \frac{E}{1 + \nu \underline{\underline{\varepsilon}}} \dot{\underline{\underline{\varepsilon}}}^p, & \text{localisation rule.} \end{array} \right. \quad (33)$$

$$\left\{ \begin{array}{ll} \dot{\underline{\underline{\varepsilon}}}^p = C \frac{\underline{\underline{S}} - \underline{\underline{b}}}{\| \underline{\underline{S}} - \underline{\underline{b}} \|}, C > 0, & \text{plastic flow,} \\ \| \underline{\underline{S}} - \underline{\underline{b}} \| = (\sigma_y - \lambda \Sigma_H) / s, & \text{yield limit,} \\ \left(\underline{\underline{S}} - \underline{\underline{b}} \right) : \left(\dot{\underline{\underline{S}}} - \dot{\underline{\underline{b}}} \right) = 0, & \text{yield limit time invariance,} \\ \dot{\underline{\underline{b}}} = \frac{kE}{E - k\underline{\underline{\varepsilon}}} \dot{\underline{\underline{\varepsilon}}}^p, & \text{kinematic hardening rule,} \\ \dot{\underline{\underline{S}}} = \text{dev} \dot{\underline{\underline{\Sigma}}} - \frac{E}{1 + \nu \underline{\underline{\varepsilon}}} \dot{\underline{\underline{\varepsilon}}}^p, & \text{localisation rule.} \end{array} \right. \quad (34)$$

$$\left\{ \begin{array}{ll} \dot{\underline{\underline{\varepsilon}}}^p = C \frac{\underline{\underline{S}} - \underline{\underline{b}}}{\| \underline{\underline{S}} - \underline{\underline{b}} \|}, C > 0, & \text{plastic flow,} \\ \| \underline{\underline{S}} - \underline{\underline{b}} \| = (\sigma_y - \lambda \Sigma_H) / s, & \text{yield limit,} \\ \left(\underline{\underline{S}} - \underline{\underline{b}} \right) : \left(\dot{\underline{\underline{S}}} - \dot{\underline{\underline{b}}} \right) = 0, & \text{yield limit time invariance,} \\ \dot{\underline{\underline{b}}} = \frac{kE}{E - k\underline{\underline{\varepsilon}}} \dot{\underline{\underline{\varepsilon}}}^p, & \text{kinematic hardening rule,} \\ \dot{\underline{\underline{S}}} = \text{dev} \dot{\underline{\underline{\Sigma}}} - \frac{E}{1 + \nu \underline{\underline{\varepsilon}}} \dot{\underline{\underline{\varepsilon}}}^p, & \text{localisation rule.} \end{array} \right. \quad (35)$$

$$\left\{ \begin{array}{ll} \dot{\underline{\underline{\varepsilon}}}^p = C \frac{\underline{\underline{S}} - \underline{\underline{b}}}{\| \underline{\underline{S}} - \underline{\underline{b}} \|}, C > 0, & \text{plastic flow,} \\ \| \underline{\underline{S}} - \underline{\underline{b}} \| = (\sigma_y - \lambda \Sigma_H) / s, & \text{yield limit,} \\ \left(\underline{\underline{S}} - \underline{\underline{b}} \right) : \left(\dot{\underline{\underline{S}}} - \dot{\underline{\underline{b}}} \right) = 0, & \text{yield limit time invariance,} \\ \dot{\underline{\underline{b}}} = \frac{kE}{E - k\underline{\underline{\varepsilon}}} \dot{\underline{\underline{\varepsilon}}}^p, & \text{kinematic hardening rule,} \\ \dot{\underline{\underline{S}}} = \text{dev} \dot{\underline{\underline{\Sigma}}} - \frac{E}{1 + \nu \underline{\underline{\varepsilon}}} \dot{\underline{\underline{\varepsilon}}}^p, & \text{localisation rule.} \end{array} \right. \quad (36)$$

$$\left\{ \begin{array}{ll} \dot{\underline{\underline{\varepsilon}}}^p = C \frac{\underline{\underline{S}} - \underline{\underline{b}}}{\| \underline{\underline{S}} - \underline{\underline{b}} \|}, C > 0, & \text{plastic flow,} \\ \| \underline{\underline{S}} - \underline{\underline{b}} \| = (\sigma_y - \lambda \Sigma_H) / s, & \text{yield limit,} \\ \left(\underline{\underline{S}} - \underline{\underline{b}} \right) : \left(\dot{\underline{\underline{S}}} - \dot{\underline{\underline{b}}} \right) = 0, & \text{yield limit time invariance,} \\ \dot{\underline{\underline{b}}} = \frac{kE}{E - k\underline{\underline{\varepsilon}}} \dot{\underline{\underline{\varepsilon}}}^p, & \text{kinematic hardening rule,} \\ \dot{\underline{\underline{S}}} = \text{dev} \dot{\underline{\underline{\Sigma}}} - \frac{E}{1 + \nu \underline{\underline{\varepsilon}}} \dot{\underline{\underline{\varepsilon}}}^p, & \text{localisation rule.} \end{array} \right. \quad (37)$$

In all cases, we get(see annex ‘Multi-dimensional analysis’)

$$\left(\underline{\underline{S}} - \underline{\underline{b}} \right) (s, t + dt) = \frac{\left(\underline{\underline{S}} - \underline{\underline{b}} \right)_{\text{trial}} (s, t + dt)}{1 + \eta}, \quad (38)$$

with

$$\eta = \max \left\{ \underbrace{0}_{\text{elastic regime}}, \underbrace{\frac{\|\underline{S} - \underline{b}\|_{\text{trial}}}{(\sigma_y - \lambda \Sigma_H)/s} - 1}_{\text{plastic regime when this number is positive}} \right\},$$

$$(\underline{S} - \underline{b})_{\text{trial}}(s, t + dt) = (\underline{S} - \underline{b})(s, t) + \text{dev} \dot{\underline{\Sigma}}(t) dt.$$

That is to say, when the structure is in elastic regime at time t and scale s , we have $(\underline{S} - \underline{b})(s, t) = (\underline{S} - \underline{b})_{\text{trial}}(s, t)$. Otherwise, if the norm of $(\underline{S} - \underline{b})_{\text{trial}}(s, t)$ is greater than the local yield limit $(\sigma_y - \lambda \Sigma_H)(1 - \tilde{D})^\delta / s$, $(\underline{S} - \underline{b})(s, t)$ will be projected on the yield limit.

Knowing the distinction between elastic and plastic regime under multiple scales, we compute the general expression of the dissipated energy rate.

$$\dot{w}(s) = (\underline{S} - \underline{b}) : \dot{\underline{\varepsilon}}^p = C \frac{(\sigma_y - \lambda \Sigma_H)}{s}. \quad (39)$$

From Eq.(A.5) and Eq.(A.8) in annex, we get:

$$E\gamma dt = \left\langle \|\underline{S} - \underline{b}\|_{\text{trial}} - \frac{(\sigma_y - \lambda \Sigma_H)}{s} \right\rangle / \left(\frac{1}{1 + \nu} + \frac{k}{E - k} \right) = \left\langle \|\underline{S} - \underline{b}\|_{\text{trial}} - \frac{(\sigma_y - \lambda \Sigma_H)}{s} \right\rangle \frac{(E - k)(1 + \nu)}{(E + k\nu)}, \quad (40)$$

where $\langle \rangle$ is Macaulay bracket symbol defined as $\langle m \rangle = 0$ if $m \leq 0$, otherwise $\langle m \rangle = m$.

We replace γ deduced from Eq.(40) in Eq.(39) to give the expression of local energy dissipation rate at scale s :

$$\dot{w}(s) dt = \frac{(E - k)(1 + \nu)}{E(E + k\nu)} \left\langle \|\underline{S} - \underline{b}\|_{\text{trial}} - \frac{(\sigma_y - \lambda \Sigma_H)}{s} \right\rangle \frac{(\sigma_y - \lambda \Sigma_H)}{s}. \quad (41)$$

With Eq.(30), the final expression of energy dissipation W during time step dt writes:

$$\begin{aligned} W &= \dot{W} dt \\ &= \frac{1}{2} \sum_i \omega_i \dot{w} \left[\left(\frac{x_i + 1}{2} \right)^{\frac{1}{1-\beta}} \right] dt \\ &= \frac{(E - k)(1 + \nu)}{2E(E + k\nu)} \sum_i \omega_i \left\langle \|\underline{S} - \underline{b}\|_{\text{trial}} - \frac{(\sigma_y - \lambda \Sigma_H)}{\left(\frac{x_i + 1}{2} \right)^{\frac{1}{1-\beta}}} \right\rangle \frac{(\sigma_y - \lambda \Sigma_H)}{\left(\frac{x_i + 1}{2} \right)^{\frac{1}{1-\beta}}}. \end{aligned} \quad (42)$$

The mean stress effect term in Chaboche model is $s_{-1} \left(1 - 3 \frac{\sigma_H}{\sigma_u} \right)$, where the fatigue limit at zero mean stress s_{-1} is reduced in the presence of σ_H . In our model, the yield limit decreases with positive mean stress.

In constant amplitude load α does not change with time. In the case of random amplitude loading history, there are two variables α and \tilde{D} in the expression of Eq.(16). We update the damage \tilde{D} at each time step as in Eq.(31).

Now we are able to put these formula into numerical tests.

5 Validation on recovery tests

5.1. Recovery of Chaboche law on cyclic loading

The test is first performed on a sinusoidal axial load $\Sigma = A\sin(t)$, giving a deviatoric amplitude $S_{max} = dev\Sigma = \left\| \sqrt{\frac{2}{3}}A\sin(t) \right\|$. We use parameters in Table 1 to recover the classic Chaboche law in cyclic loading.

Parameters	Value
Young's modulus	$E = 72$ GPa
Hardening parameter	$k = 600$ MPa
Weakening scales distribution exponent	$\beta = 1.75$
Hydrostatic pressure sensitivity	$\lambda = 0.3$
Macroscopic yield stress	$\sigma_y = 230$ MPa
Sequencing effect sensitivity	$a = 0.5$
Dissipated energy to failure per unit volume	$W_0 = 3$ MJ(MPa)

Table 1: Material parameters in a simple cyclic load

We use matlab to realize our analytical method. We plot $\left\| \underline{\underline{S}} - \underline{\underline{b}} \right\|_{trial}$ and $\left\| \underline{\underline{S}} - \underline{\underline{b}} \right\|$ at two different scales ($s_{33} = 4.20$ and $s_{40} = 9.68$) in Figure 6 and Figure 7. The local yield limit is reduced in the presence of positive hydrostatic stress whereas negative ones have beneficial effects.

The dissipated energy per time step is depicted in Figure 8 with its enlargement in Figure 9. We scale S_{max} in the plot to see more clear the relation between energy dissipation and stress intensity. The “jump” in energy evolution is due to activation of new scales while in-between two scales the dissipated energy follows the stress increment at each time step. α does not affect the dissipated energy W , only concerns damage accumulation rate.

The accumulated energy dissipation without damage accumulation law is shown in Figure 10. The difference between analytical energy loss and numerical one is shown in Figure 11. The damage evolves like in Figure 12, where we compare the damage evolution as predicted by the cycle accumulation Eq.(7) and by the numerical strategy of section 4.

Now we compare the result to the one demonstrated in Figure 3. We can see from Figure 13 the difference between cyclic load calculation and numerical method as function of time steps n . From the relative difference figure we conclude that the two methods converge.

There is discrepancy between analytical damage and numerical damage calculation at the beginning, this is due to the numerical implementation difference that the analytical result is calculated by equally dividing the W_{cyc} into 200 time steps in one cycle leading to constant dissipation per time step, whilst the numerical result is instantaneously calculated at each time step following stress evolution. So the numerical damage

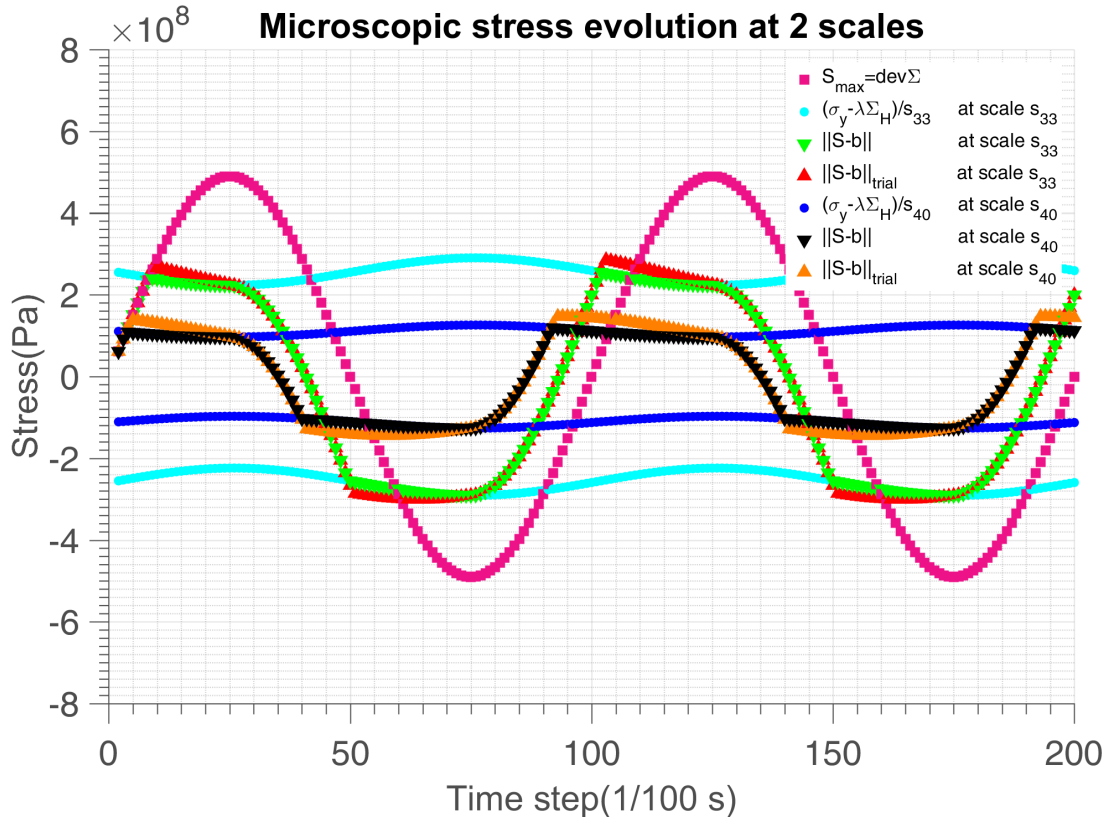


Figure 6: Microscopic $(\underline{\underline{S}} - \underline{\underline{b}})_{trial}$ and $(\underline{\underline{S}} - \underline{\underline{b}})$ evolution with time under different weakening scales ($s_{33} = 4.20$ and $s_{40} = 9.68$) in sinusoidal load with zero mean stress

accumulation line swings around the analytical line. The relative difference is significant at the beginning but becomes negligible as number of steps gets larger.

The cyclic load calculation is only valid for very simple such as proportional loading in fatigue, nevertheless it can still be used as a comparison group to verify the numerical results. The outcome seems satisfactory. Hence, to be more general for any loading history, we adopt the numerical method.

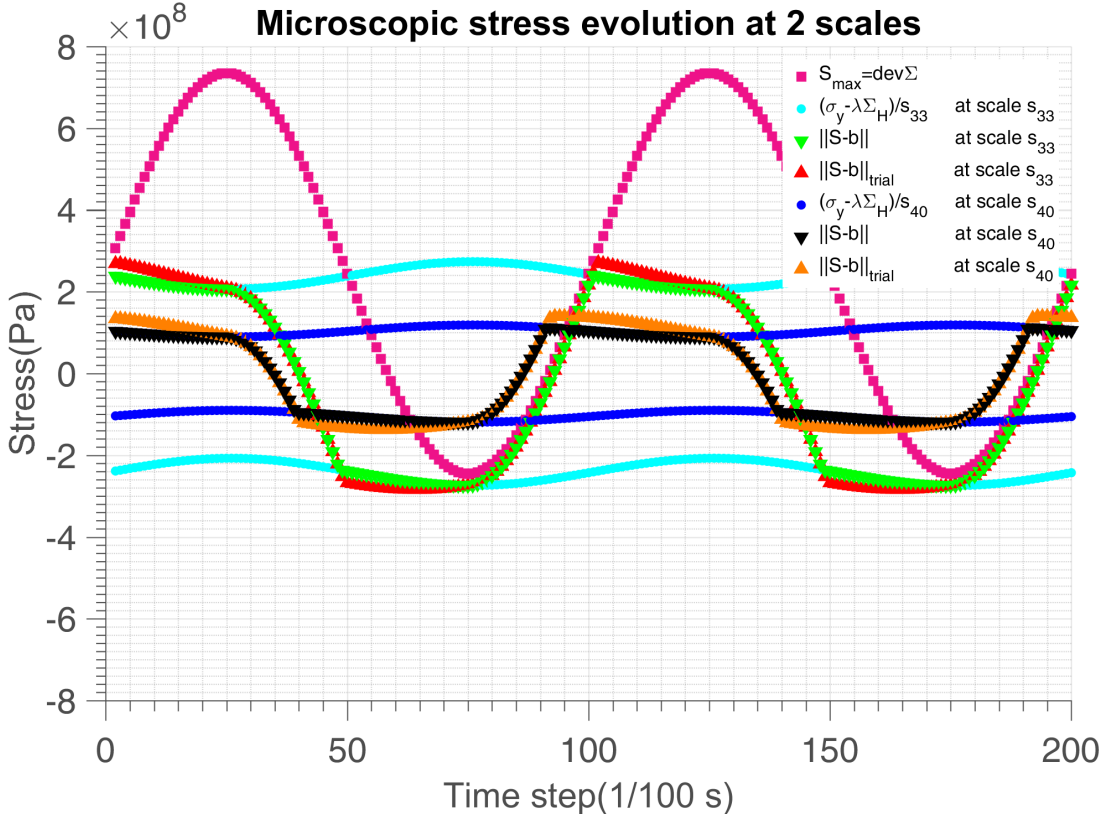


Figure 7: Microscopic $(\underline{\underline{S}} - \underline{\underline{b}})_{trial}$ and $(\underline{\underline{S}} - \underline{\underline{b}})$ evolution with time under different weakening scales ($s_{33} = 4.20$ and $s_{40} = 9.68$) in sinusoidal load with non-zero mean stress

5.2. Numerical recovery of sequence effect

We adopt the parameter α to take into account the sequence effect. The high-low loading sequence clearly reduces the fatigue life, as depicted in Figure 14. In order to cover this phenomenon, we let α change with time. Here α is the sequence effect sensitivity, according to Eq.(22), we have:

$$s_{min}(t) = \frac{\sigma_y - \lambda \Sigma_H(t)}{S_{max}(t)},$$

which is the minimum weakening scale that activates energy loss. We use a general law for α of the type $\alpha = \alpha(s_{min})$ with the idea that for us s_{min} is a measure of present intensity of macroscopic stress = mechanical based stress norm.

Numerically we review our method of the sequence effect as depicted in Figure 14.

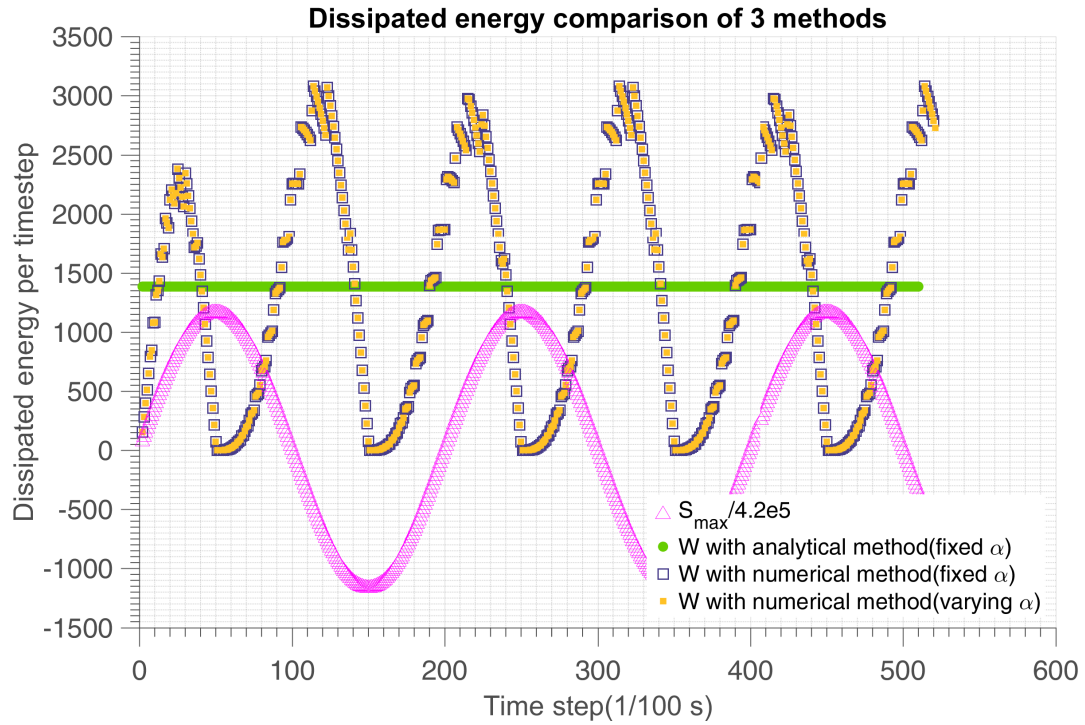


Figure 8: Validation of dissipated energy in all scales with analytical and numerical method

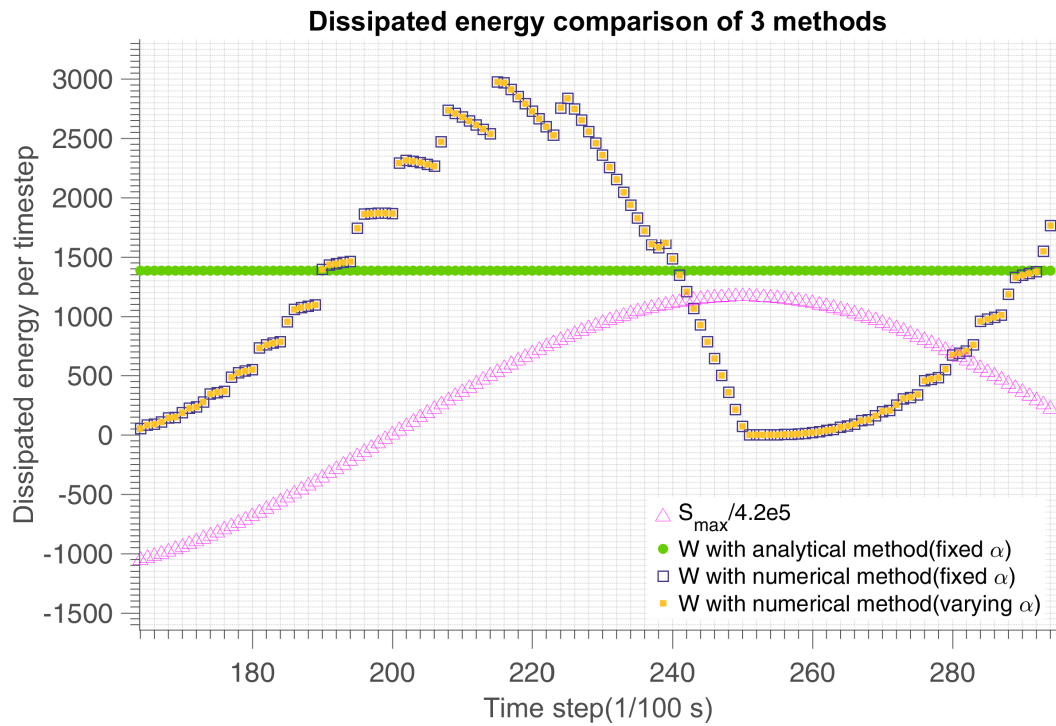


Figure 9: Partial enlargement of Figure 8

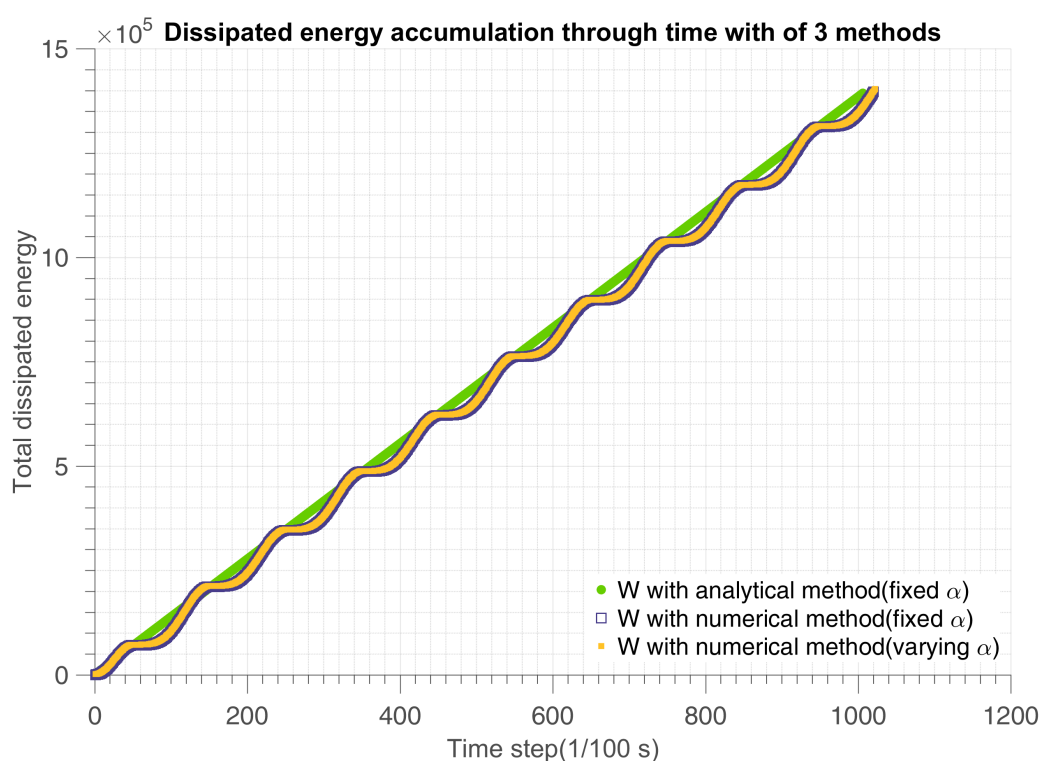


Figure 10: Dissipated energy accumulation through time with of 3 methods

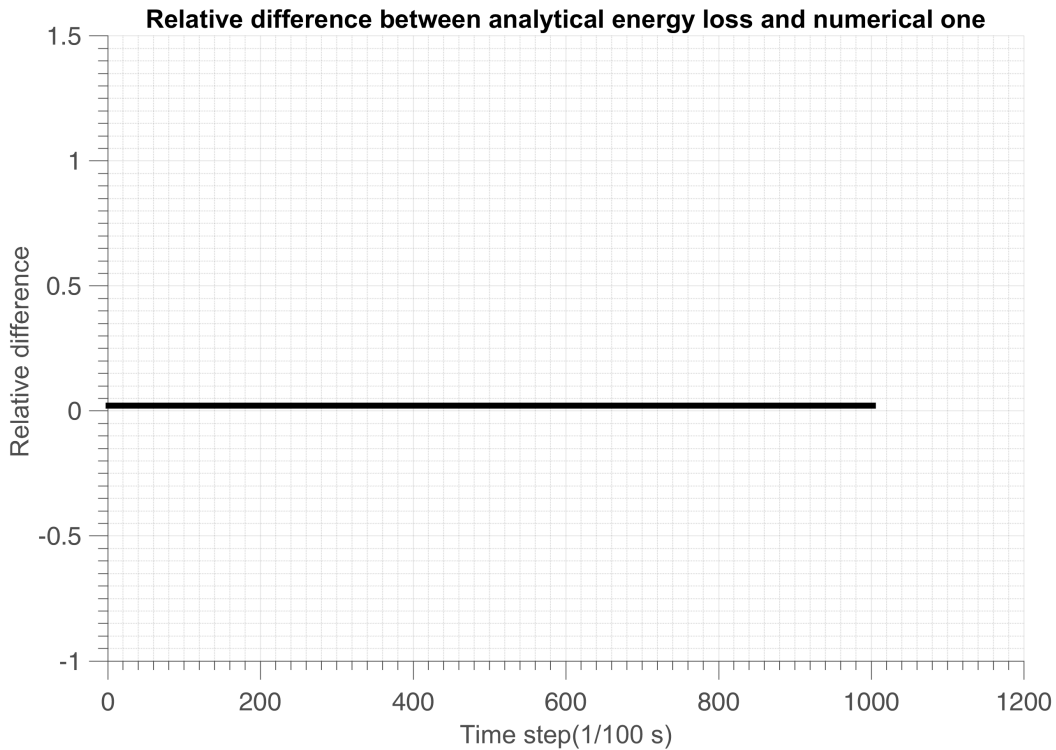


Figure 11: Relative difference $\frac{W_{analytical} - W_{numerical}}{W_{analytical}}$ between analytical energy loss and numerical one with α varying with time

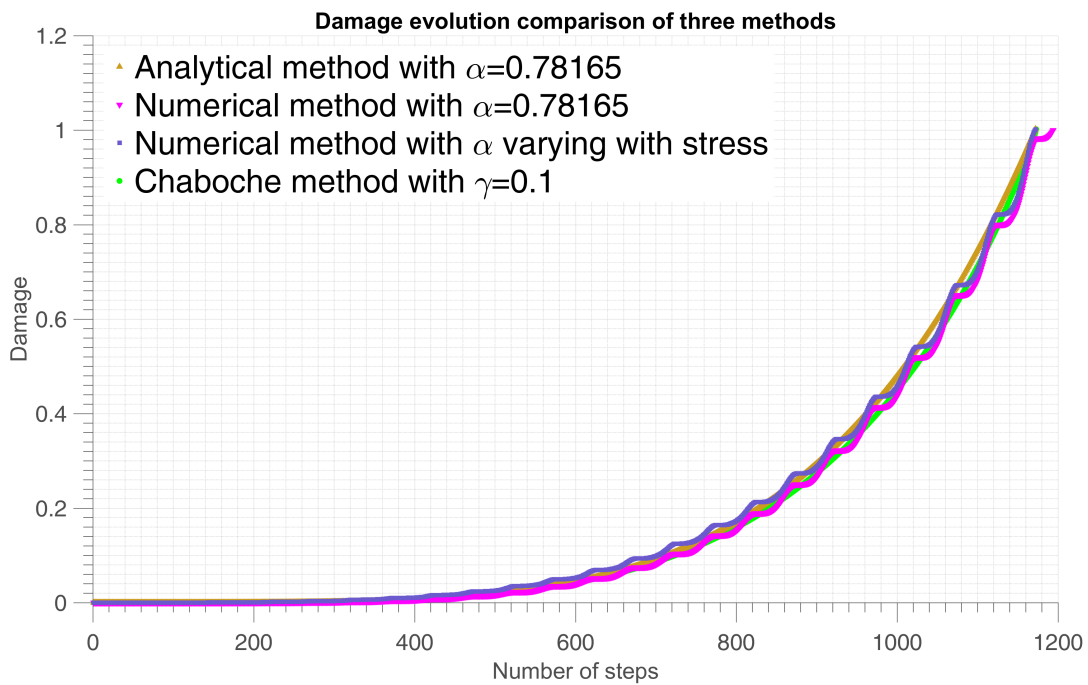
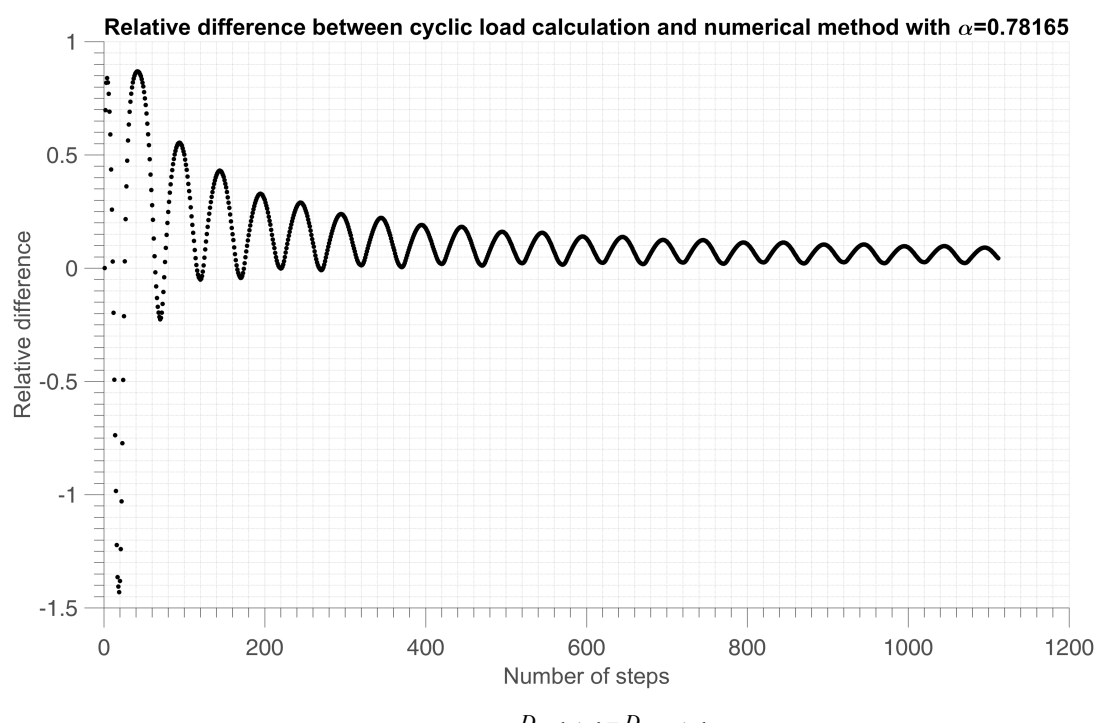


Figure 12: Damage evolution with time under sinusoidal load with two different methods



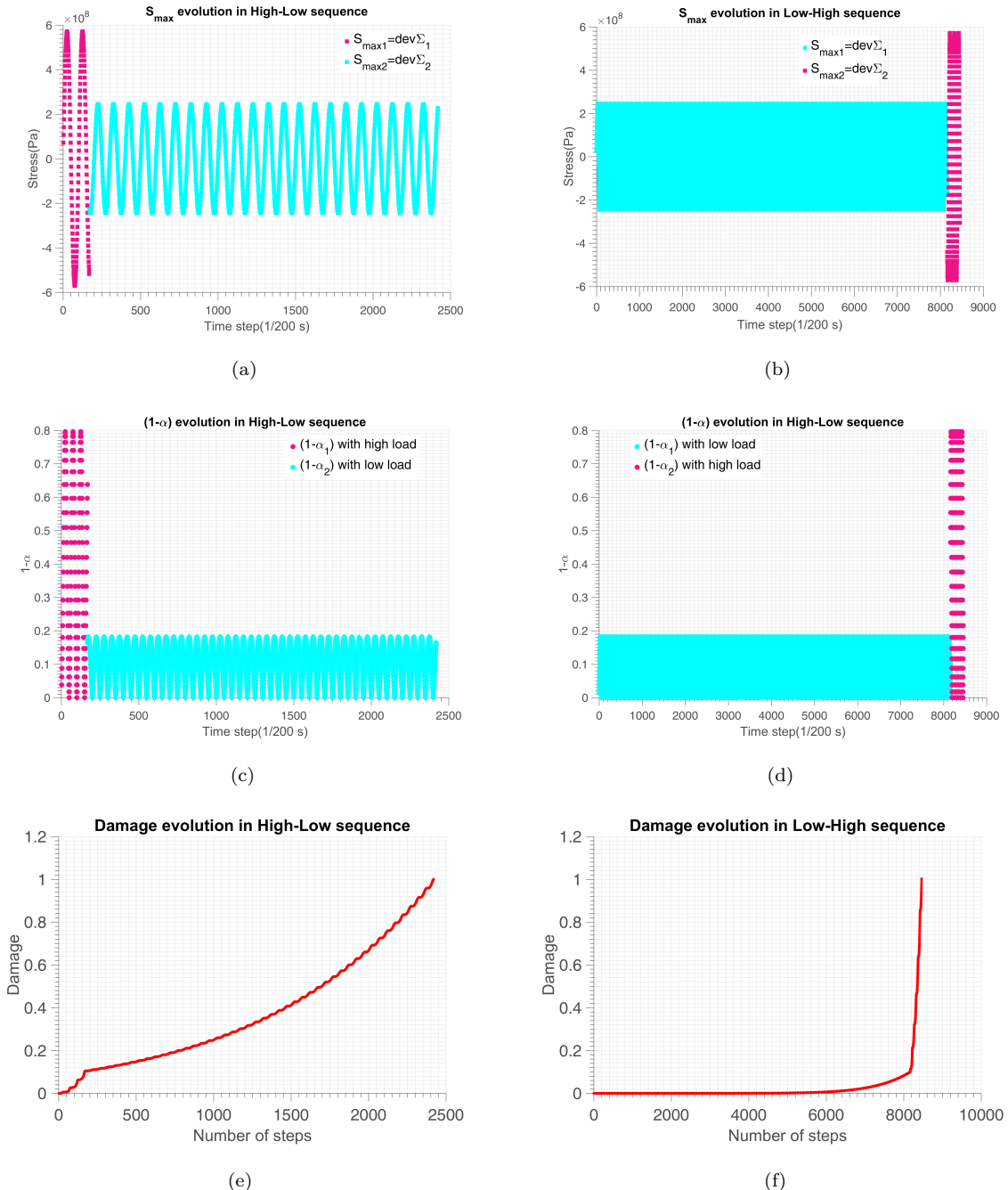


Figure 14: Two level sequence effect.

6 Experimental verification

6.1. Constant amplitude 1D tests from Cetim on AW-6106 T6 aluminum

The tests are performed on aluminum batches, the characteristics of the sample are shown in table 2.

Specimen geometry for fatigue and corrosion fatigue tests ($t < 3.5$ mm):

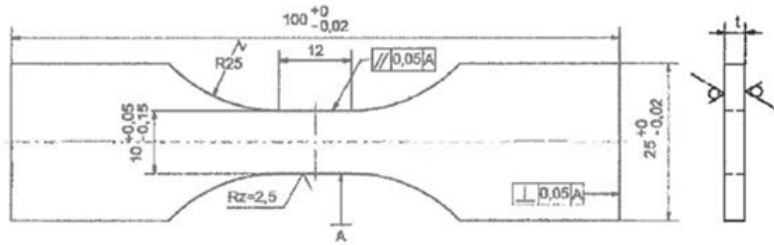


Figure 15: Specimen geometry for fatigue tests of AW-6106 T6 aluminum

Parameters	Value
Young's modulus	$E = 72$ GPa
Hardening parameter	$k = 8.5$ MPa
Macroscopic yield stress	$\sigma_y = 230$ MPa
Thickness	$e = 2.9$ mm
Width	$l = 9.95$ mm

Table 2: Material parameters

Comparison of fixed and varying α with constant amplitude loading

The parameters we introduced during the deduction need to be calibrated. The source of the parameter identification are listed in Table 5. In the case of constant amplitude loading, analytically α does not change with time because S_{max} is a linear function of stress intensity. However, numerically α changes with time because real life experiments have fluctuations. The comparison with the average α are shown in Figure 16. The relative error of number of points to failure n_F is 0.142%.

For instance in constant amplitude loading, the number of cycles to failure according to Eq.(15) with fixed α is expressed as Eq.(43):

$$\begin{aligned}
 N_F &= \frac{W_0}{(1 - \alpha) W_{cyc}} \\
 &= \frac{W_0}{(1 - \alpha)} \frac{E(E + kv)\beta(\beta + 1)}{4(E - k)(1 + v)(\beta - 1)} \frac{(\sigma_y - \lambda \Sigma_H)^{\beta-1}}{S_{max}^{\beta+1}}.
 \end{aligned} \tag{43}$$

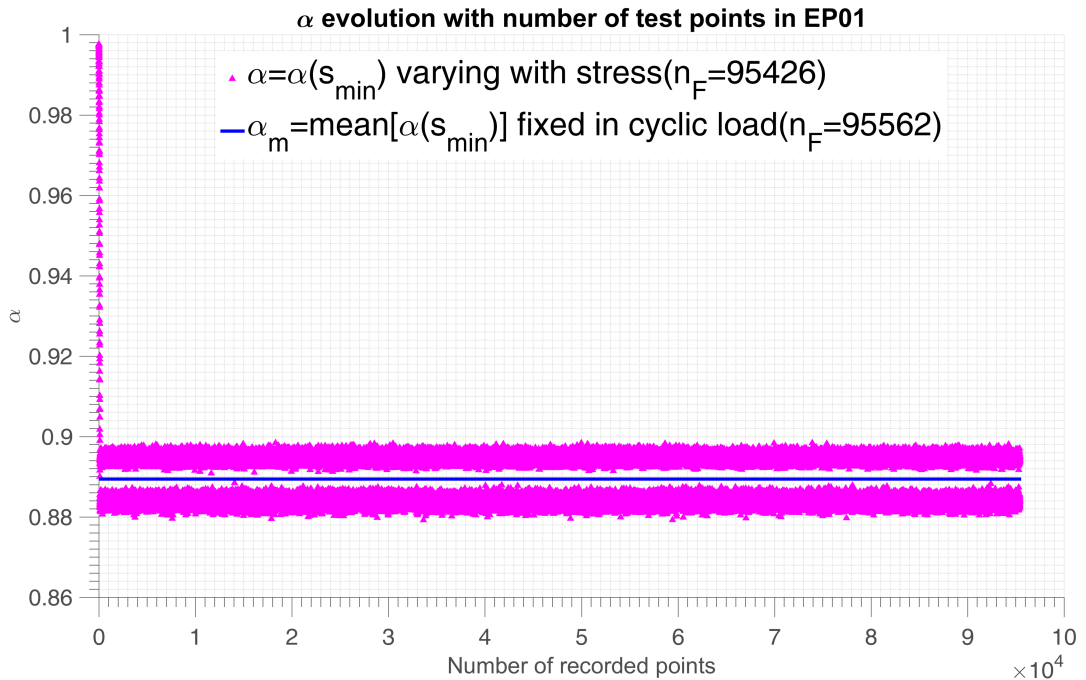


Figure 16: Different choice of alpha numerically

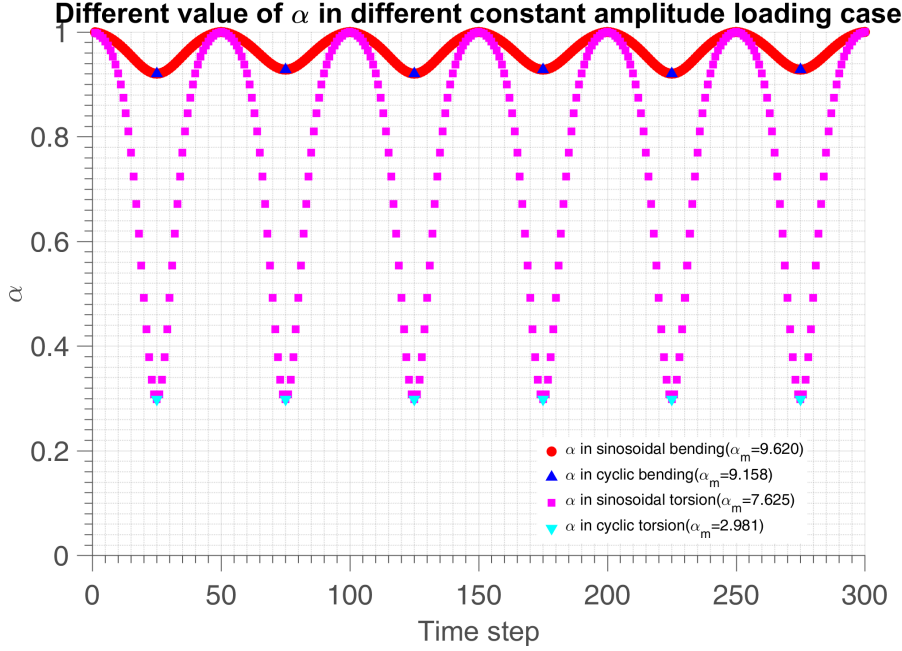
We now apply this formulation to a simple cyclic load with mean stress m applied on aluminum having $\Sigma_y = 230\text{ MPa}$.

$$\Sigma(n) = A \sin(\pi/2 + n\pi) + m.$$

Which gives $\Sigma_{max} = A + m$ and $\Sigma_{min} = -A + m$. We give $m = 0.1A$. $S_{max} = \sqrt{\frac{2}{3}}A$ in cyclic loading is the amplitude of deviatoric stress and independent from mean stress m .

Where n is the number of recorded points. Similar as shown in Figure 16 with negligible error, in $S - N$ curve there is only cyclic loading with constant amplitude, so we analytically use the mean value of α for the damage accumulation part and $(\sigma_y - \lambda \Sigma_H)_m$ for the energy dissipation part through one cycle to give N_F at each point in $S - N$ curve. However, α_m is not fixed with constant amplitude of loading case, it depends on the loading pattern. Normal stresses act to pull parallel planes within the material apart or push them closer together, while shear stresses act to slide planes along one another. Normal stresses promote crack formation and growth, while shear stresses underlie yield and plastic slip.

Published data on the yield strength of steels and other structural materials is typically limited to values determined from uniaxial tension tests. The yield strength is customarily defined as that value of tensile stress which when relaxed to zero results in an unrecovered strain of 0.2%. The torsional yield strength (τ_y) is generally assumed to be 0.5–0.6 of this tensile value, based on one or another of the several popular theories of plasticity[6]. Here we give two methods to get α_m as shown in Figure 17.

Figure 17: Comparing different calculation methods of α_m

We have in damage accumulation part as in Eq.(44):

$$\alpha_m = \frac{\alpha(s_{min1}) + \alpha(s_{min2})}{2} = \frac{[1 - \alpha(s_{min1} - 1)^{-\beta}] + [1 - \alpha(s_{min2} - 1)^{-\beta}]}{2}, \quad (44)$$

with

$$s_{min1} = \frac{\left(\sigma_y - \lambda \frac{\Sigma_{max}}{3}\right)}{S_{max}},$$

$$s_{min2} = \frac{\left(\sigma_y - \lambda \frac{\Sigma_{min}}{3}\right)}{S_{max}}.$$

The mean parameter we give concerning the energy dissipation part is:

$$(\sigma_y - \lambda \Sigma_H)_m = \frac{\left(\sigma_y - \lambda \frac{\Sigma_{max}}{3}\right) + \left(\sigma_y - \lambda \frac{\Sigma_{min}}{3}\right)}{2} = \sigma_y - \lambda \frac{m}{3}.$$

This deduction give the mean value of dissipated energy in one cycle in constant amplitude loading as in Eq.(45):

$$W_{cycm} = \frac{4(E - k)(1 + \nu)(\beta - 1)}{E(E + kv)\beta(\beta + 1)} \frac{S_{max}^{\beta+1}}{\left(\sigma_y - \lambda \frac{m}{3}\right)^{\beta-1}}. \quad (45)$$

The final expression to validate cyclic loading experiments is expressed as in Eq.(46).

$$N_F = \frac{W_0}{(1 - \alpha_m) W_{cycm}}. \quad (46)$$

Once α_m is fixed in constant amplitude cyclic loading, this parameter has the same influence as W_0 . The parameters remain to calibrate are λ on the mean stress sensitivity and distinction between bending and torsion, β on the slope of $S - N$ curve.

What should we use for S_{max} in the presence of mean stress? The amplitude or the mean value of $\{\max, \min\}$? I used the later method in the fitting of 30NCD16, SM45C and 10HNAP steel: The stress tensor $\underline{\underline{\sigma}}$ is then:

$$\underline{\underline{\sigma}}(t) = \begin{pmatrix} \sigma_a \sin(\omega t) + m & \tau_a \sin(\omega t) & 0 \\ \tau_a \sin(\omega t) & 0 & 0 \\ 0 & 0 & 0 \end{pmatrix}. \quad (47)$$

with deviator

$$\underline{\underline{S}} = \underline{\underline{\sigma}} - \frac{1}{3} \text{tr} \underline{\underline{\sigma}} = \begin{pmatrix} \frac{2}{3} (\sigma_a \sin(\omega t) + m) & \tau_a \sin(\omega t) & 0 \\ \tau_a \sin(\omega t) & -\frac{1}{3} (\sigma_a \sin(\omega t) + m) & 0 \\ 0 & 0 & -\frac{1}{3} (\sigma_a \sin(\omega t) + m) \end{pmatrix}. \quad (48)$$

Here I use:

$$S_{max} = \text{mean}(\sqrt{\underline{\underline{S}}^2}).$$

The method of take the mean values of α , σ_y and S_{max} analytically in the presence of mean stress or in the case of multiaxial loading is not feasible here. We propose in constant amplitude load it is necessary to numerically calculate the mean values of α and W_{cycm} through several cycles and apply the result via Eq.(46). The assumption is for constant amplitude loading the energy dissipation is time independent as shown in Figure 10. In this way the numerical cost is neither as high as step by step numerical implementation in random amplitude loading case, nor inaccurate as analytical mean value method.

6.2. Random amplitude 1D tests from Cetim on AW-6106 T6 aluminum

There are 12 validated uniaxial fatigue tests on the AW-6106 T6 aluminum sample, in which 2 are constant amplitude load case and 10 random load case. The cyclic stress of test number 1(ep01) and test number 2(ep02) are respectively 131.9MPa and 97.0MPa. We first identify the same parameters feasible to both loading cases.

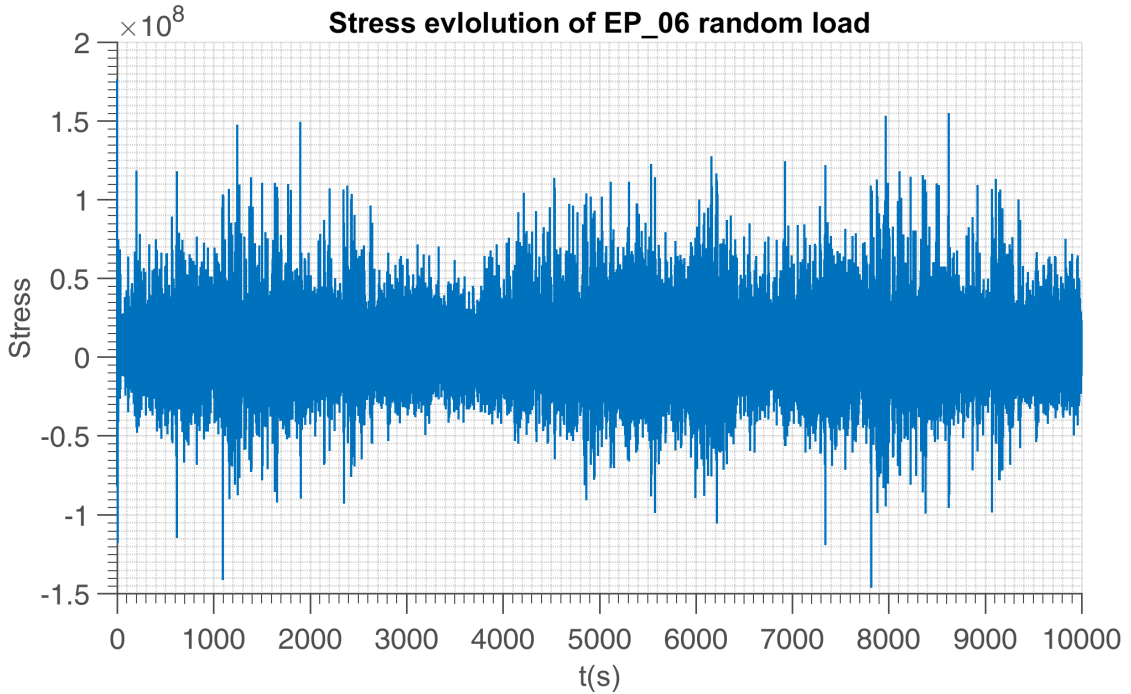


Figure 18: Random loading history on batch 06 of AW-6106 T6 aluminum

The detailed tests information are shown in table 3. There are $27000(\pm 2.4\%)$ recorded points per repetition.

We assume the material parameters like Young's modulus, hardening parameter, hydrostatic pressure sensitivity, macroscopic yield stress, Wohler curve exponent and sequence effect parameters are known. We first identify the weakening scales distribution, and dissipated energy to failure from cyclic tests ep01 and ep02. Then change the parameter n_0 to see if our assumption is correct or need to be changed.

The numerical fitting process show that the damage is caused mainly by large stresses. The definition of major stress now need to be specified according to the material. To take into account this effect we first find out the proportion stress above a certain value in the repetition signal of random loading, as shown in Table 4. Here ep_a and ep_b are the same material. Since the samples were extracted from aluminum profiles of industrial production, the two batches only correspond to two different times of sampling in the production. The variation is supposed to be representative of the regular tolerances you might have in

Specimen	Fmax (kN)	Σ_{max} in the block	Number of repetition	Number of points
BATCH_A_01	3.375			99892
BATCH_A_02	2.475			414298
BATCH_A_04	nom	225.88	95	2500000
BATCH_A_05	nom	225.88	156	4105263
BATCH_A_06	nom	225.88	145	3815789
BATCH_A_07	nom	225.88	90	2368421
BATCH_A_08	nom	225.88	194	5105263
BATCH_A_09	nom	225.88	197	5184211
BATCH_A_10	nom x 0,9	203.292	515	13552632
BATCH_A_11	nom x 0,9	203.292	385	10131579
BATCH_A_12	nom x 0,9	203.292	424	11157895
BATCH_A_13	nom x 0,9	203.292	409	10763158
BATCH_B_01	nom	225.88	121	3184211
BATCH_B_02	nom x 0,8	180.704	380	10000000
BATCH_B_03	nom x 0,8	180.704	380	10000000
BATCH_B_04	nom x 0,9	203.292	406	10684211
BATCH_B_05	nom x 0,9	203.292	454	11947368
BATCH_B_06	nom x 0,9	203.292	518	13631579
BATCH_B_07	nom x 0,9	203.292	553	14552632
BATCH_B_08	nom x 0,9	203.292	612	16105263
BATCH_B_09	nom	225.88	253	6657895
BATCH_B_10	nom	225.88	196	5157895
BATCH_B_11	nom	225.88	178	4684211
BATCH_B_12	nom	225.88	123	3236842

Table 3: Cetim fatigue tests result on AW-6106 T6 aluminum

the production. ep_a_01 and ep_a_02 are constant amplitude loading which helps identify the power of weakening scale distribution β . ep_a_03 is low cycle fatigue data. ep_b_02 and ep_b_03 have infinite life time. The data in the table are grabbed from random signal high cycle fatigue loading history.

Parameter sensitivity analysis

The tests on uniaxial loading of a certain material needs a fixed set of parameters. We first perform a sensitivity analysis to see the influence of each parameter.

We analyze the sensitivity of parameters separately as in Table 6 and Table 7. The parameter β has more

Stress>	70	90	110	130	150	170	190
$S_{max}>$	57.15	73.48	89.81	106.14	122.47	138.80	155.13
X	0.497	0.639	0.781	0.923	1.065	1.207	1.349
ep_a_04	1.962%	0.904%	0.077%	0.037%	0.018%	0.007%	
ep_a_05	1.604%	0.784%	0.044%	0.030%	0.007%	0.007%	
ep_a_06	1.645%	0.784%	0.045%	0.030%	0.007%	0.007%	
ep_a_07	1.632%	0.788%	0.048%	0.029%	0.007%	0.007%	
ep_a_08	1.644%	0.787%	0.048%	0.037%	0.007%	0.007%	
ep_a_09	1.655%	0.800%	0.048%	0.037%	0.007%	0.007%	
ep_a_10	0.768%	0.134%	0.007%	0.000%	0.000%	0.000%	
ep_a_11	0.772%	0.145%	0.007%	0.000%	0.000%	0.000%	
ep_a_12	0.779%	0.133%	0.011%	0.000%	0.000%	0.000%	
ep_a_13	0.775%	0.141%	0.007%	0.000%	0.000%	0.000%	
ep_b_01	4.739%	1.737%	0.840%	0.224%	0.049%	0.034%	0.004%
ep_b_04	1.999%	0.745%	0.156%	0.034%	0.004%	0.000%	0.000%
ep_b_05	2.010%	0.749%	0.148%	0.034%	0.008%	0.000%	0.000%
ep_b_06	1.999%	0.790%	0.118%	0.034%	0.008%	0.000%	0.000%
ep_b_07	2.029%	0.756%	0.152%	0.034%	0.008%	0.000%	0.000%
ep_b_08	1.999%	0.737%	0.137%	0.034%	0.008%	0.000%	0.000%
ep_b_09	4.663%	1.687%	0.798%	0.205%	0.049%	0.034%	0.004%
ep_b_10	4.712%	1.744%	0.809%	0.224%	0.046%	0.034%	0.004%
ep_b_11	4.636%	1.664%	0.790%	0.209%	0.049%	0.034%	0.004%
ep_b_12	0.775%	0.141%	0.007%	0.000%	0.000%	0.000%	0.000%

Table 4: Proportion of major damage stress applied(MPa) where $\Sigma_y=230\text{MPa}$, test on AW-6106 T6 aluminum.

influence on the random loading case because it acts not only as the S-N curve slope but also the power magnification factor of large stress intensity. The λ has little influence because both tests are conducted on very small or zero mean stress load history.

In Miner's law the parameter α is zero, the maximum value is below 1. For $\alpha = 1$ the damage accumulation line becomes flat and there is unlimited lifetime. To keep α in the range of $\{0, 1\}$ where in random amplitude tests there is $S_{max} = 163.3\text{MPa}$. We have the sensitivity of load intensity a ranging from 0.1 to 0.29 to give α positive value. To assess large stress correctly we define the larger stress intensity as:

$$S_{large} > \frac{\Sigma_y}{2}.$$

Parameters	Strategy
Hardening parameter k	material constant
Macroscopic yield stress σ_y	material constant
Hydrostatic pressure sensitivity λ	hydrostatic stress sensitivity
Non-linearity of damage accumulation a	amplification factor of load intensity
Weakening scales distribution exponent β	to be calibrated
Dissipated energy to failure per defect W_0	energy scaling

Table 5: Parameters concerned

The weakening scale distribution exponent(also the slope of S-N curve of the material) β ranges from 1 to 5. The hydrostatic pressure sensitivity λ is from positive mean stress test, which has the range of $0 \sim 0.8$. In constant amplitude cyclic loading, the dissipated energy to failure per defect W_0 (in MPa) is related to fatigue lifetime of the material.

Constant,amplitude sensitivity test with $f(\beta) = \beta$							
	Ref	Min	Max	Ref_n	Min_n	Max_n	Sensitivity
β	1.1	1.05	1.50	414233	783723	243300	-3.19
λ	0.1	0.05	0.50	414233	449598	443376	0.00
W_0	3.27e8	1.00e8	5.00e8	414233	137498	687209	1.08
a	0.1	0.05	0.15	414233	672869	324754	-0.84

Table 6: Parameters sensitivity at cyclic loading of ep02 on AW-6106 T6 aluminum

Random amplitude sensitivity test with $f(\beta) = \beta$							
	Ref	Min	Max	Ref_n	Min_n	Max_n	Sensitivity
β	1.1	1.05	1.50	4220452	7469257	1799585	-3.28
λ	0.1	0.05	0.50	4220452	4566335	2175991	-0.13
W_0	3.27e8	1.00e8	5.00e8	4220452	1321761	6420810	0.99
a	0.1	0.05	0.15	4220452	7156622	2827894	-1.03

Table 7: Parameters sensitivity at random loading of ep05 on AW-6106 T6 aluminum

From Table.8 and Table.9 we can see $f(\beta)$ has positive correlation with β in high cycle fatigue which is the regime we focus on. So we give $f(\beta) = \beta$ in high cycle random loading case to minimize the parameters to collaborate. The sensitivity of parameters is calculated with Eq.(49).

Constant amplitude sensitivity test with $f(\beta) \neq \beta$							
	Ref	Min	Max	Ref_n	Min_n	Max_n	Sensitivity
β	1.1	1.05	1.50	414233	797377	213682	-3.44
λ	0.1	0.05	0.50	414233	449598	443376	0.00
W_0	3.27e8	1.00e8	5.00e8	414233	137498	687209	1.08
a	0.1	0.05	0.15	414233	672869	324754	-0.84
$f(\beta)$	1.1	1.05	1.5	414233	441661	511644	0.41

Table 8: Parameters sensitivity at cyclic loading of ep02 on AW-6106 T6 aluminum

Random amplitude sensitivity test with $f(\beta) \neq \beta$							
	Ref	Min	Max	Ref_n	Min_n	Max_n	Sensitivity
β	1.1	1.05	1.50	4220452	7254554	2472791	-2.77
λ	0.1	0.05	0.50	4220452	4566335	2175991	-0.13
W_0	3.27e8	1.00e8	5.00e8	4220452	1321761	6420810	0.99
a	0.1	0.05	0.15	4220452	7156622	2827894	-1.03
$f(\beta)$	1.1	1.05	1.5	4220452	4341560	3052299	-0.75

Table 9: Parameters sensitivity at random loading of ep05 on AW-6106 T6 aluminum

$$sensitivity = \frac{(Max_n - Min_n) / Ref_n}{(Max - Min) / Ref}. \quad (49)$$

The standard S-N curve is fitted with fatigue data provided by Cetim(the red line). Analytical calculation of mean dissipated energy and of the average value of α on one cycle, and integration of the differential equation in D with these mean values is provided. The comparison with numerical method where we have changing α and W at each time step in standard $S - N$ curve is shown in Figure 19:a. This analytical strategy is proposed to give a much cheaper way to treat cyclic loadings for high cycle fatigue.

The influence of all the parameters on constant amplitude cyclic load using Eq.(43) are shown in Figure 19.

The different parameters impacts are shown in purple curves. We can see the weakening scale β changes the inclination of S-N curve. β is also the magnification factor which magnify large stress damage as well as minify small stress damage. Not surprisingly the hydrostatic stress sensitivity λ has more influence on large stress. The amplification factor of load intensity in damage accumulation a and energy scaling in damage accumulation law W_0 adapts to fatigue life without changing the shape the S-N curve.

6.2.1. Major damage effect

The α parameter has crucial influence on the damage accumulation on different stress intensities. In Figure 20 we can see α value and damage accumulation speed as function of life proportion. The range of α is $[-\infty, 1]$ but the negative values of α lost its physical meaning for the damage accumulation becomes slower at the later stage of fatigue. From Eq.(20) we can draw the evolution of damage with different α to see its influence on the accumulation law.

To see the influence of sequence effect factor of α , we first fix $\alpha = 0.7$ for all tests to see the results. When α is fixed, it becomes denominator in the final expression of N_F (Eq.(43)) and has the same impact as W_0 . We find out that the fatigue life of random loading is widely dispersed as in . In this case we need to use $\alpha = f(s_{min})$ which evolves with time to make large stress intensity deal more damage.

After analysis we find out that large stresses cause much more damage than the smaller stresses, even with α in Eq.(24) the standard deviation is big. So it is necessary to include this major stress induced damage to our stress intensity parameter α .

With the new α compared to Eq.(24) we are able to calibrate our model better with the experimental results.

$$\alpha = 1 - a \left(\frac{\frac{1}{s_{min}}}{1 - \frac{1}{s_{min}}} \right)^{f(\beta)}.$$

We use the power $f(\beta)$ related to energy dissipation parameter β to magnify large stress impact and minify lower stress damage. The demonstration of major damage effect using $f(\beta)$ is depicted in Figure 21. With larger value of $f(\beta)$, high stress causes more damage and low stress cause less damage.

Here the power $f(\beta)$ and has anti-correlation with T_F in low cycle fatigue regime but has positive correlation in high cycle fatigue regime. In our work the HCF is the regime we concern, so it is physically logical to give:

$$f(\beta) = \beta.$$

which yields the new expression of α in Eq.(50):

$$\alpha = 1 - a (s_{min} - 1)^{-\beta}. \quad (50)$$

The larger value of S_{max} causes more damage in the presence of the power β , leading to faster increase of

$$(1 - \alpha) = a \left(\frac{\frac{1}{s_{min}}}{1 - \frac{1}{s_{min}}} \right)^\beta$$

which causes faster damage accumulation. We can also see this effect in Figure ???. However, α must be positive.

The parameters used in the fitting process are shown in Tab.???. The deviatoric stress S_{max} , above which the damage is magnified, is determined from:

$$S_{large} = \frac{1}{2} \Sigma_y.$$

This major damage effect can be seen in Figure 22.

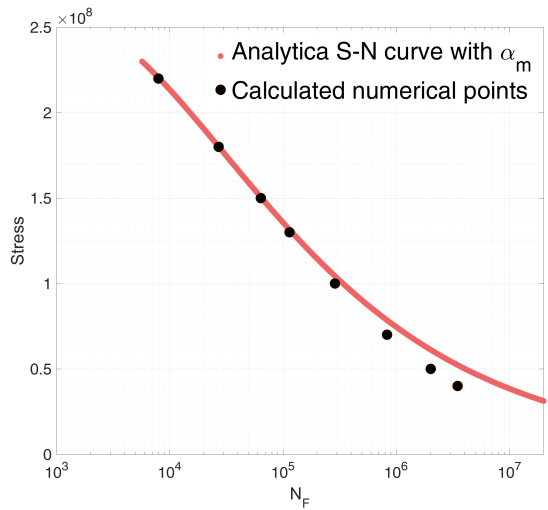
The reference parameters value we use are in Tab.10.

Constant α	W_0 (MPa)	λ	β	α
	326.9	0.1	1.1	0.7
Changing α	W_0 (MPa)	λ	β	α
	326.9	0.1	1.1	0.1

Table 10: The parameters in 1D cyclic and random loading on AW-6106 T6 aluminum fatigue tests by Cetim

The best fitted results with constant α are shown in Figure 23. The dispersion is relatively large. In conclusion, we are not able to predict the random stress amplitude fatigue life with fixed α , because random stresses not only cause different energy dissipations, but also have influence on damage accumulation speed, so we have to update the value of α at each time step.

We can find that the numerical results are satisfactory with magnification power. The dispersion figure with distinction of major damage is depicted in Figure 24. Here it is necessary to control the parameter α to make sure $\alpha > 0$ in the most severe situation.



(a) S-N curve using numerical and analytical method

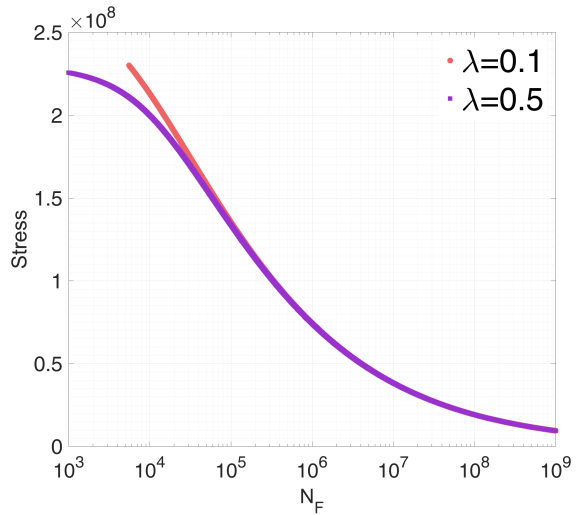
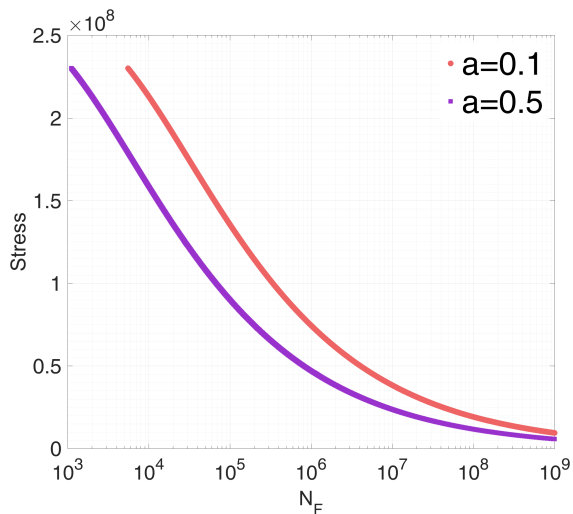
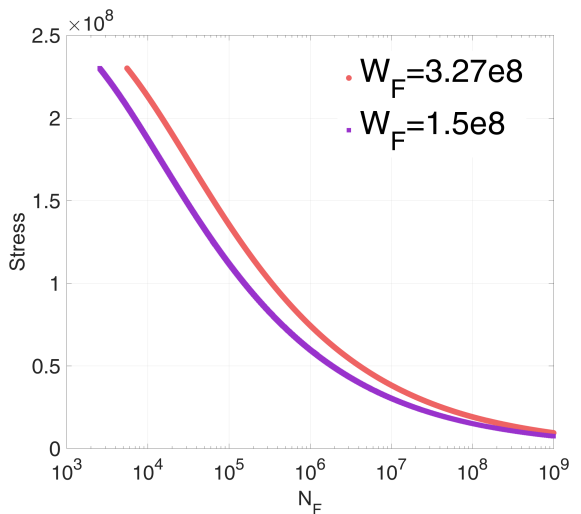
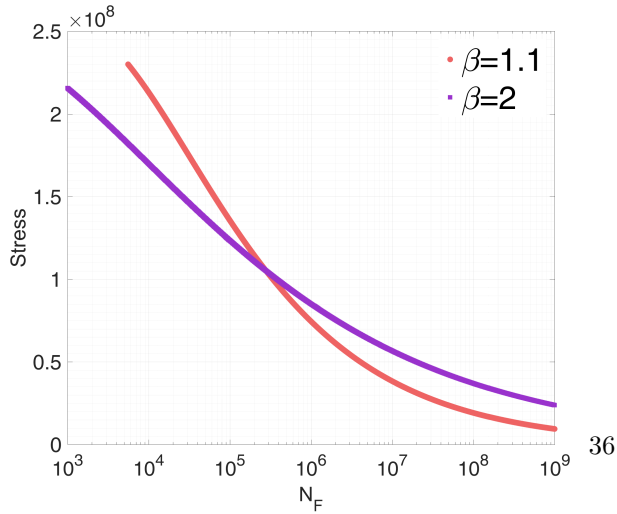
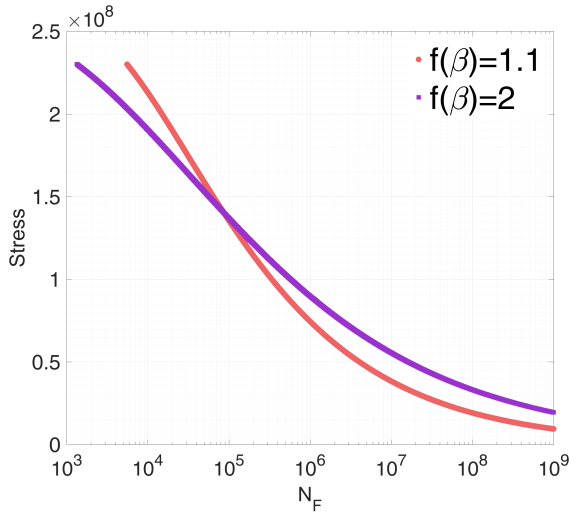
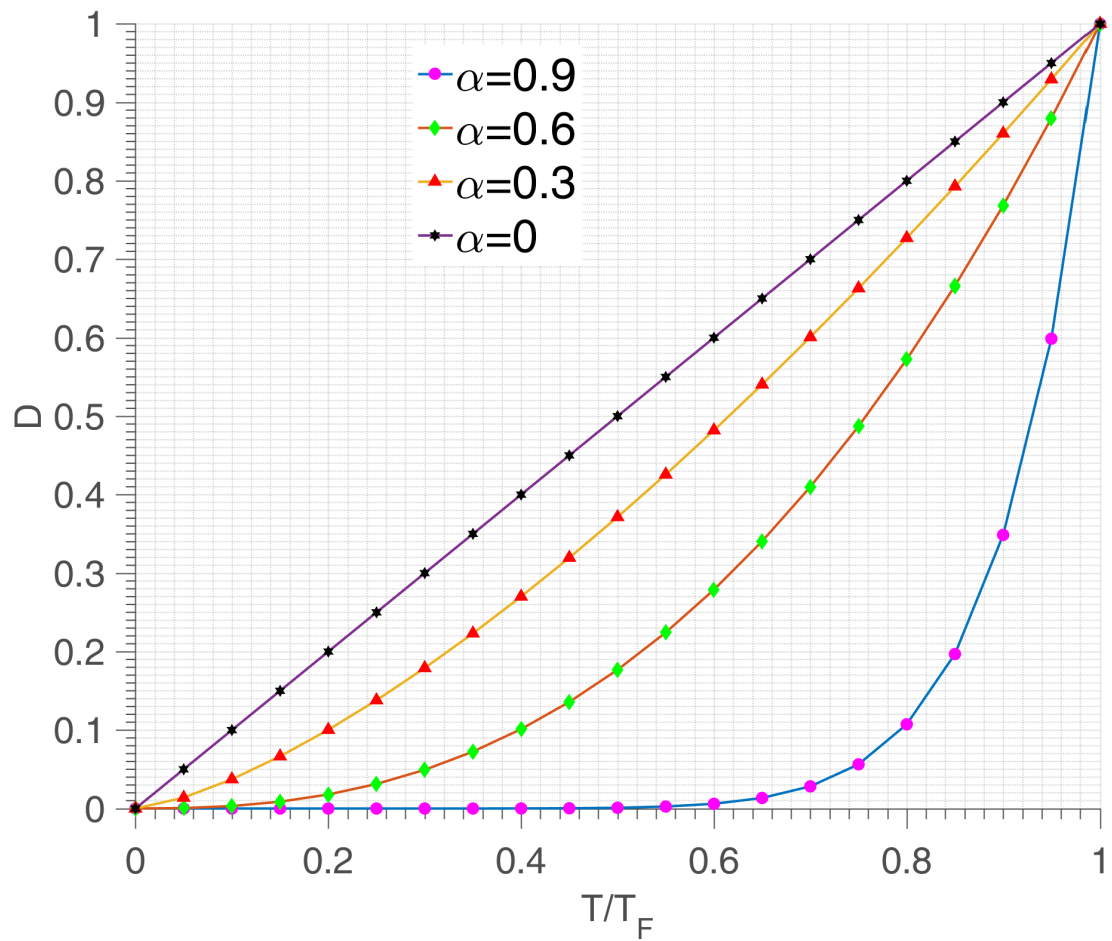
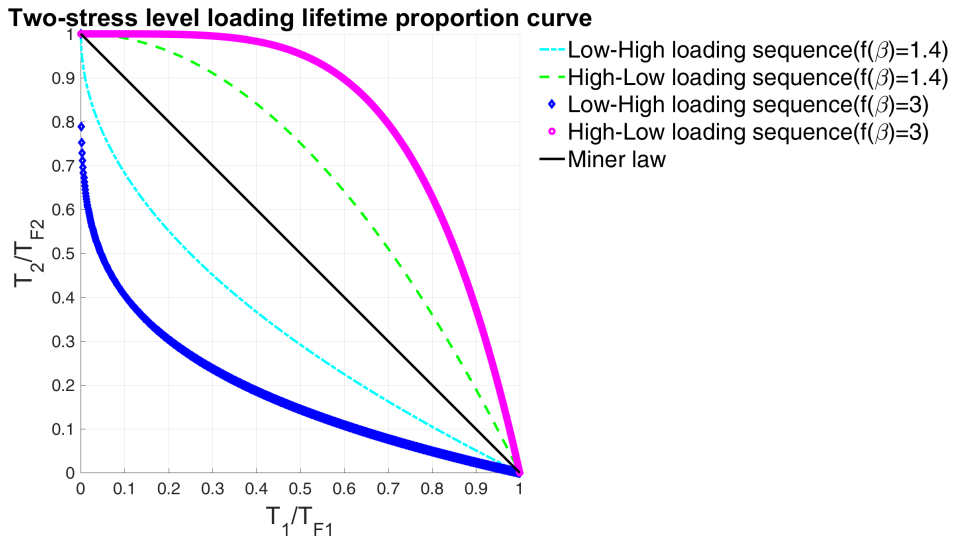
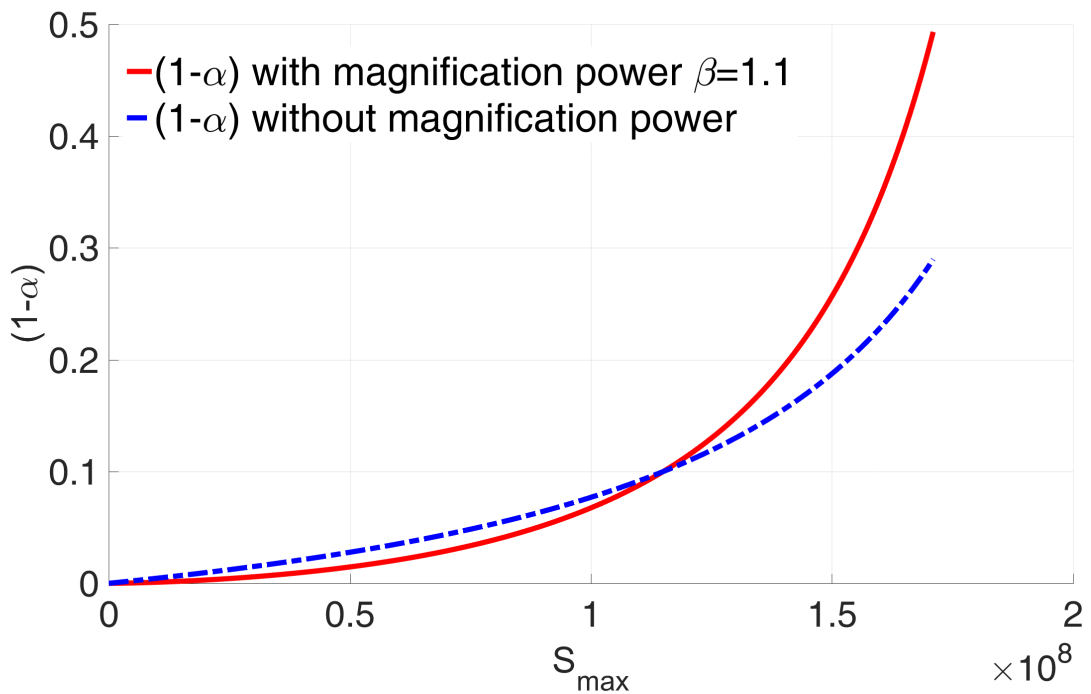
(b) The λ influence on S-N curve(c) The α influence on S-N curve(d) The W_F influence on S-N curve(e) The β influence on S-N curve(f) The $f(\beta)$ influence on S-N curve

Figure 19: The influence of parameters on the shape and limit of S-N curve

Figure 20: Influence of α on damage accumulation

Figure 21: Major damage effect using different $f(\beta)$ on sequence effect figureFigure 22: $(1-\alpha)$ term with and without the magnification power β

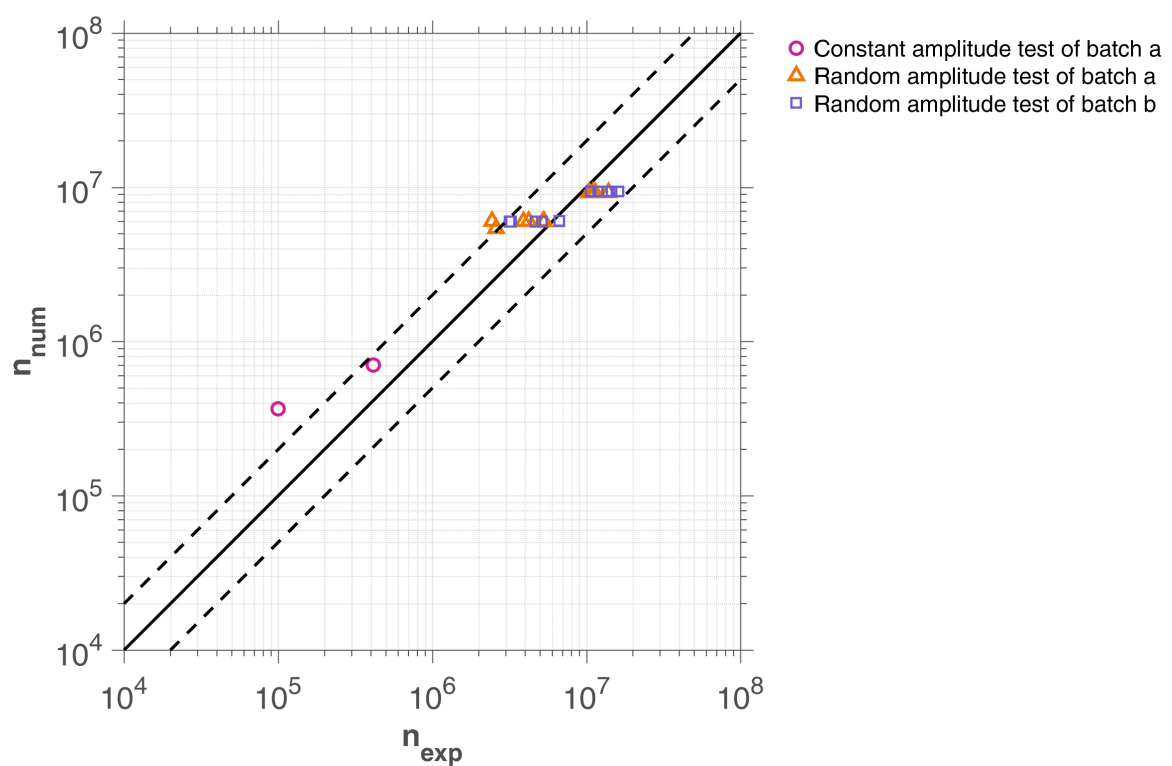


Figure 23: Comparison between experimental and numerical results of 1D cyclic and random loading on aluminum fatigue tests by Cetim with constant α

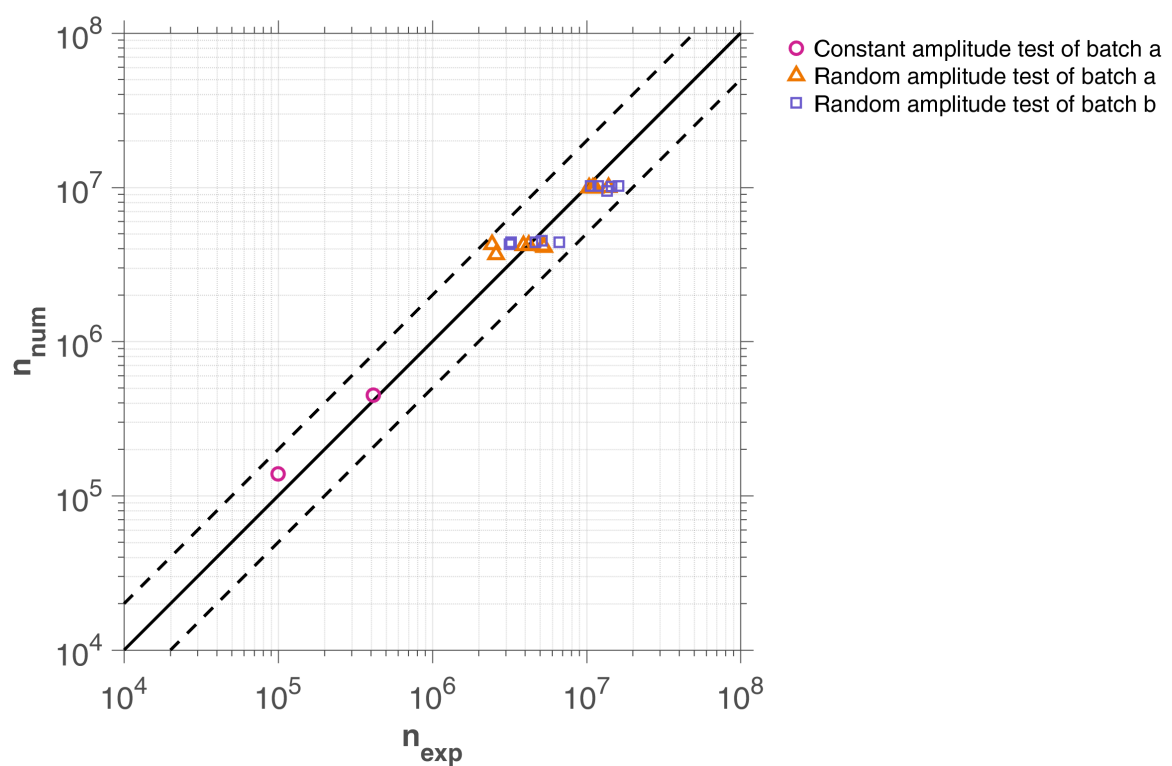


Figure 24: Comparison between experimental and numerical results of 1D cyclic and random loading on aluminum fatigue tests by Cetim

6.3. Experimental validation of the model on 30NCD16 steel

6.3.1. Presentation of steel 30 NCD 16

Tests with blocks of loading from database are compared to our model predictions. The material for testing is steel 30NCD16. The mechanical characteristics relating to each lot were determined by Dubar [7] by effecting monotonic tensile test batch. He eventually define “average material” one who has characteristics listed in Table. 11:

$\sigma_{y0.02\%}$ [MPa]	$\sigma_{y0.2\%}$ [MPa]	σ_u [MPa]	σ_{-1} [MPa]	τ_{-1} [MPa]	E [GPa]
895	1080	1200	690	428	191

Table 11: Mechanical and dynamic characteristics of 30NCD16 steel [7]

6.3.2. Fatigue tests performed by Dubar on steel 30 NCD 16

Tests carried out under simple bending and torsional stresses are grouped together in Table. 12 and 13.

Bending Tests (R=-1)	N [Cycles]	$\sigma_{x,m}$ [MPa]	$\sigma_{x,a}$ [MPa]
1	51000	0	820
2	80000	0	795
3	90000	0	790
4	95000	0	785
5	100000	0	780
6	120000	0	765
7	140000	0	752
8	200000	0	725
9	210000	0	720
10	230000	0	715
11	250000	0	708
12	51000	450	640
13	140000	450	620
14	120000	290	695
15	250000	290	660

Table 12: 30NCD16 steel fully reversed bending tests [7]

Torsion Tests (R=-1)	N [Cycles]	$\tau_{xy,a}$ [MPa]
16	51000	527
17	80000	505
18	90000	500
19	95000	497
20	100000	495
21	120000	482
22	140000	470
23	200000	450
24	210000	446
25	230000	445
26	250000	440

Table 13: 30NCD16 steel fully reversed torsion tests [7]

The results of combined bending-torsion tests in phase with or without mean stress $\sigma_{x,m}$ are given in the following table:

Bending Tests (R=-1)	N [Cycles]	$\sigma_{x,m}$ [MPa]	$\sigma_{x,a}$ [MPa]	$\tau_{xy,a}$ [MPa]
27	51000	0	600	335
28	80000	0	548	306
29	90000	290	0	460
30	95000	450	0	460
31	100000	450	0	430
32	120000	450	490	285
33	140000	290	500	290

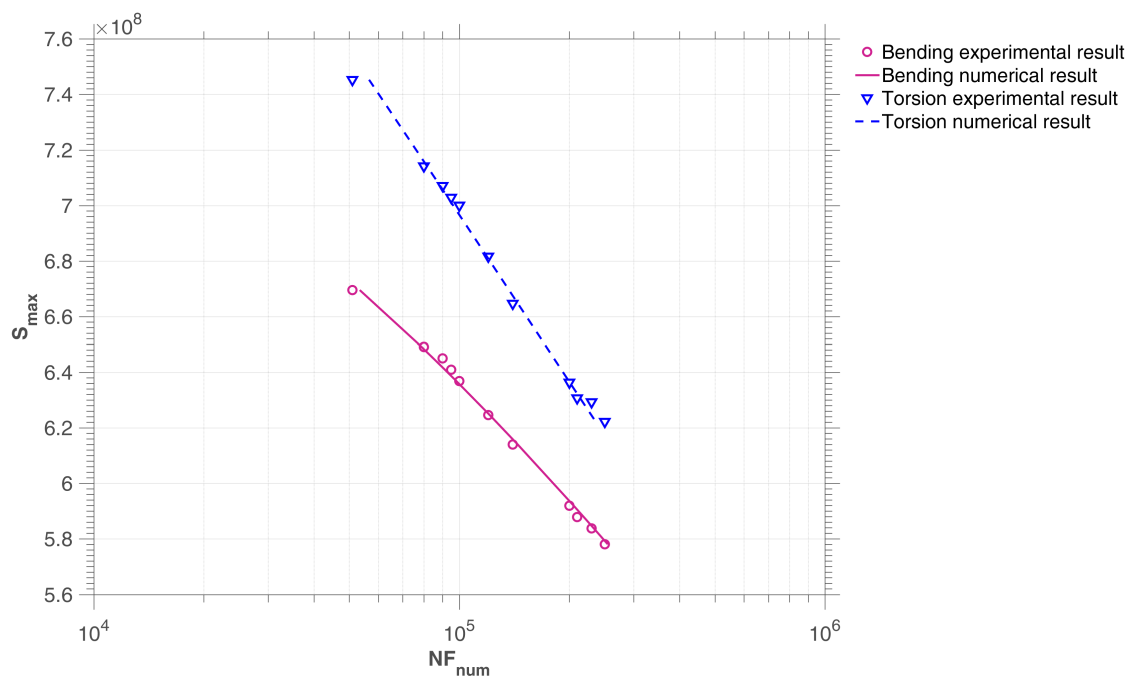
Table 14: 30NCD16 steel bending-torsion tests [7]

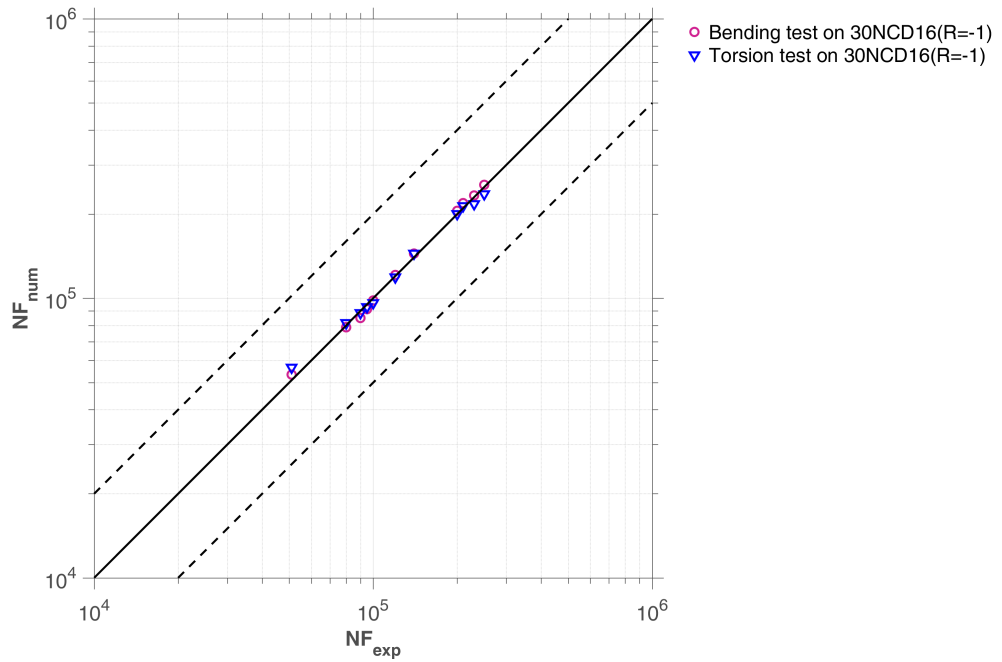
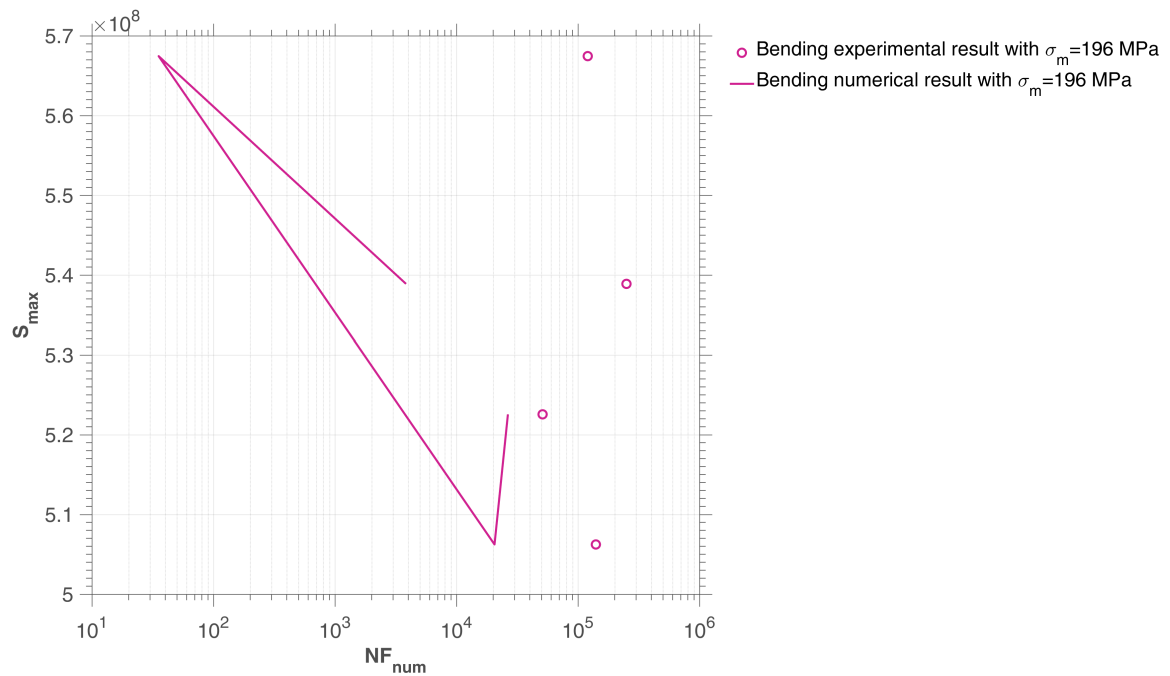
6.3.3. Identification of model parameters for steel 30 NCD 16

Indeed, the identification of the parameters consists in minimizing the relative difference between the experimental lifetimes and calculated for purely alternating bending tests (R = -1). This is clearly indicated in figure (3.13) by obtaining a good correlation between these different lifetimes

β	λ	W_0/a
1.85	0.85	440e9

Table 15: Parameter identification of 30NCD16 steel

Figure 25: Bending and torsion tests on 30NCD16($R=-1$)

Figure 26: Bending and torsion tests on 30NCD16($R=-1$)Figure 27: Bending tests with mean stress on 30NCD16($R=-1$)

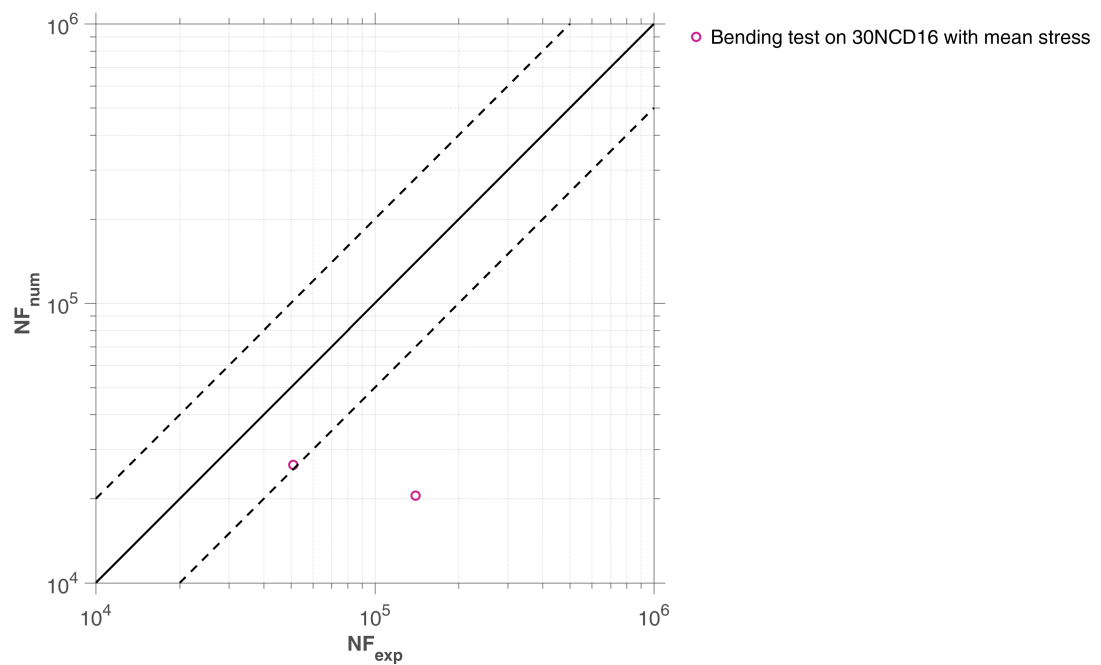
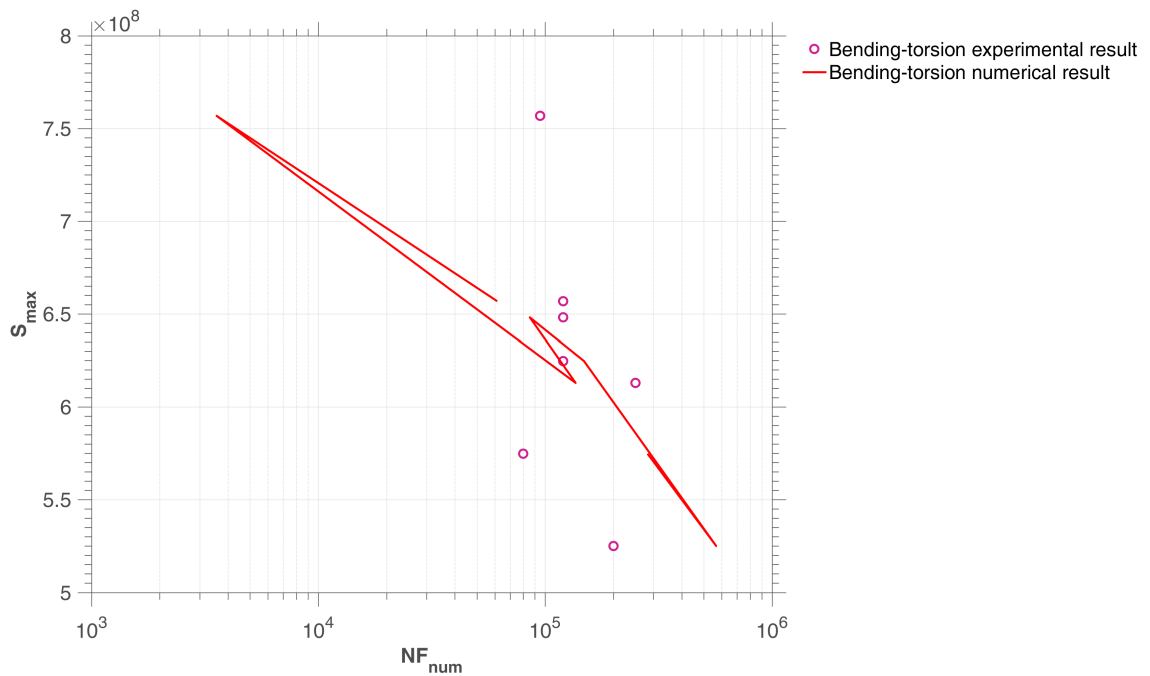
Figure 28: Bending tests with mean stress on 30NCD16($R=-1$)

Figure 29: Bending-torsion tests with mean stress on 30NCD16

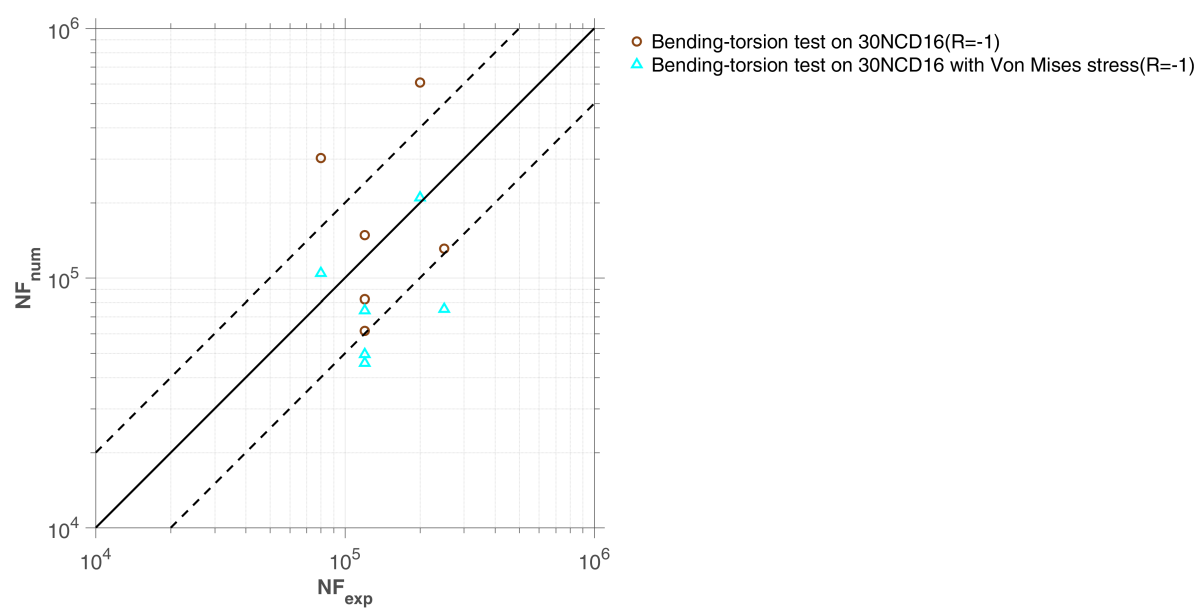


Figure 30: Bending-torsion tests with mean stress on 30NCD16

6.4. Experimental validation of the model on SM45C steel

6.4.1. Presentation of steel SM45C

This is a structural steel widespread use for the crankshafts and the structural components. The chemical composition and mechanical properties of this material is given in Table. 16 and Table. 17.

C	Mn	P	S	Si	Ni	Cr	Cu
0.42	0.73	0.02	0.012	0.28	0.14	0.18	0.13

Table 16: Chemical composition of SM45C steel

σ_y [MPa]	σ_u [MPa]	E [GPa]	G [GPa]	ν	A
638	824	213	82.5	0.29	22

Table 17: Mechanical and dynamic characteristics of SM45C steel

E: Young's modulus,

G: Shear modulus,

ν : Poisson ratio,

A: Elongation at break.

6.4.2. Fatigue tests performed by Dubar on steel SM45C

Preliminary fatigue tests in purely alternating torsion and purely alternating flexion were performed by Lee [8]. These two types of tests were carried out with test pieces of the same geometric shape. In addition, the author had performed moderate stress bending fatigue tests to study its effect on the lifetime of SM45C steel. All uniaxial fatigue tests performed by Lee [8] are illustrated in Figure 31. This figure shows a reduction in bending life of SM45C steel in the presence of a positive mean stress. Crack initiation was detected when the stiffness of the specimen or specimen used was reduced by 10%.

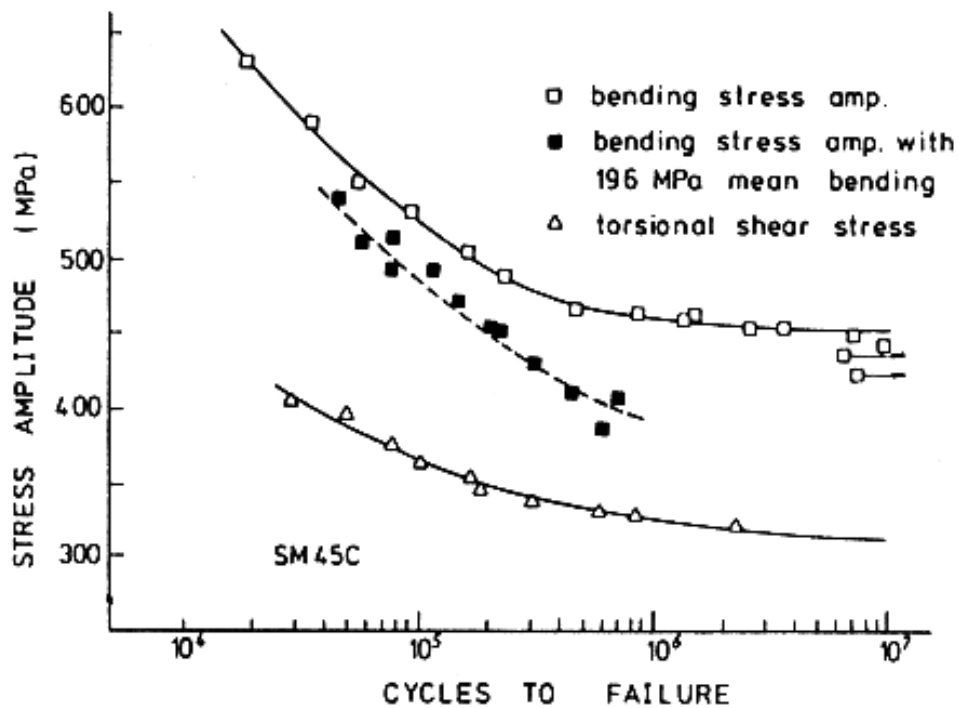


Figure 31: Fatigue curves made on SM45C steel by Lee [8]

Preliminary fatigue tests were carried out under fully reversed bending and torsion separately.

In the case of multiaxial bending-torsion block tests (Table. 20), we could alternatively adopt Von Mises stress as the value of S_{max} :

$$S_{max} = \sigma_{von} = \sqrt{\frac{1}{2} [(\sigma_{xx} - \sigma_{yy})^2 + (\sigma_{yy} - \sigma_{zz})^2 + (\sigma_{zz} - \sigma_{xx})^2] + 3(\tau_{xy}^2 + \tau_{yz}^2 + \tau_{zx}^2)} \quad (51)$$

Bending Tests R=-1	N [Cycles]	$\sigma_{x,a}$ [MPa]	$\sigma_{x,m}$ [MPa]
1	1.9E4	620	0
2	3.6E4	590	0
3	5.8E4	552	0
4	9E4	535	0
5	1.7E5	505	0
6	2.2E5	490	0
7	4.4E5	470	0
8	8E5	465	0
9	1.4E6	462	0
10	1.5E6	465	0
11	2.4E6	460	0
12	3.3E6	460	0
13	6E6	440	0
14	6.6E6	458	0
15	7E6	430	0
16	9E6	448	0
17	4.5E4	540	196
18	5.4E4	515	196
19	7E4	520	196
20	7.1E4	485	196
21	1.1E5	485	196
22	1.5E5	475	196
23	2E5	460	196
24	2.1E5	455	196
25	3E5	435	196
26	4.3E5	415	196
27	6.9E5	410	196
28	5.8E5	390	196

Table 18: SM45C steel fully reversed bending tests(extracted from [8])

Torsion Tests R=-1	N [Cycles]	$\tau_{xy,a}$ [MPa]
1	2.9E4	405
2	5E4	399
3	7.8E4	380
4	1E5	365
5	1.8E5	355
6	1.9E5	349
7	3E5	340
8	5.8E5	335
9	8.2E5	333
10	2.25E6	325

Table 19: SM45 steel fully reversed torsion tests(extracted from [8])

6.4.3. Identification of model parameters for steel SM45C

We use the Von Mises yield strength combining the bending and torsion yield limits as σ_y . The fitted curve using experimental data in Table. 20 and data with mean stress effect is shown in Figure ???. The tests on SM45C steel have illustrated that the mean bending stress has an influence on both uniaxial and multiaxial fatigue life.

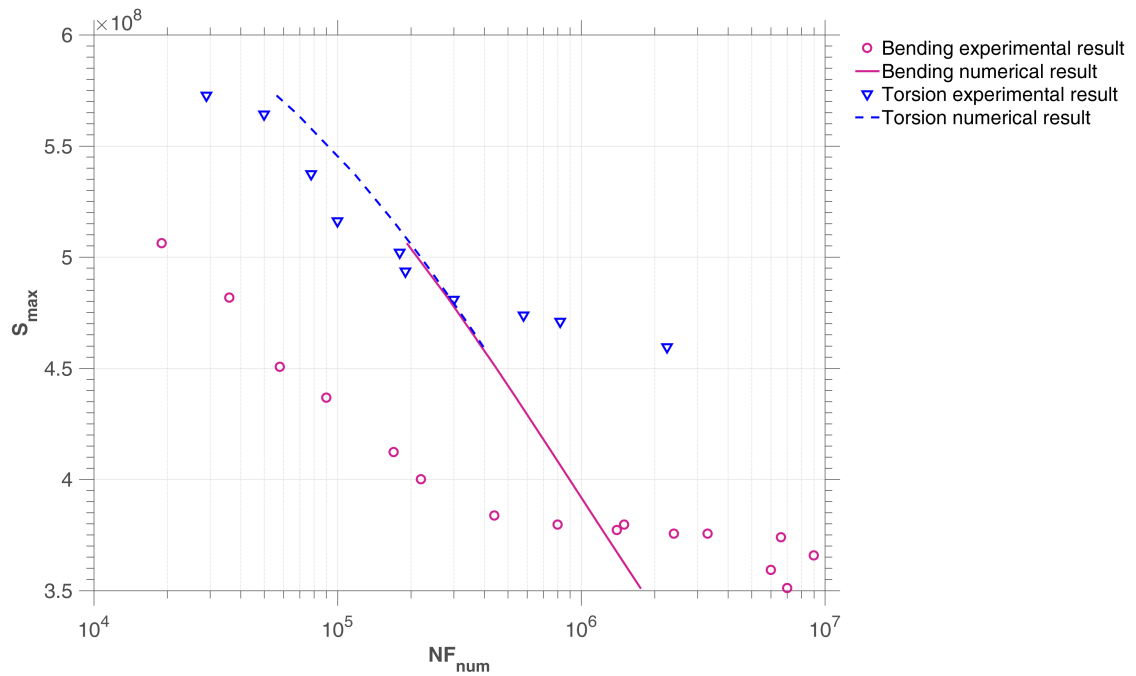
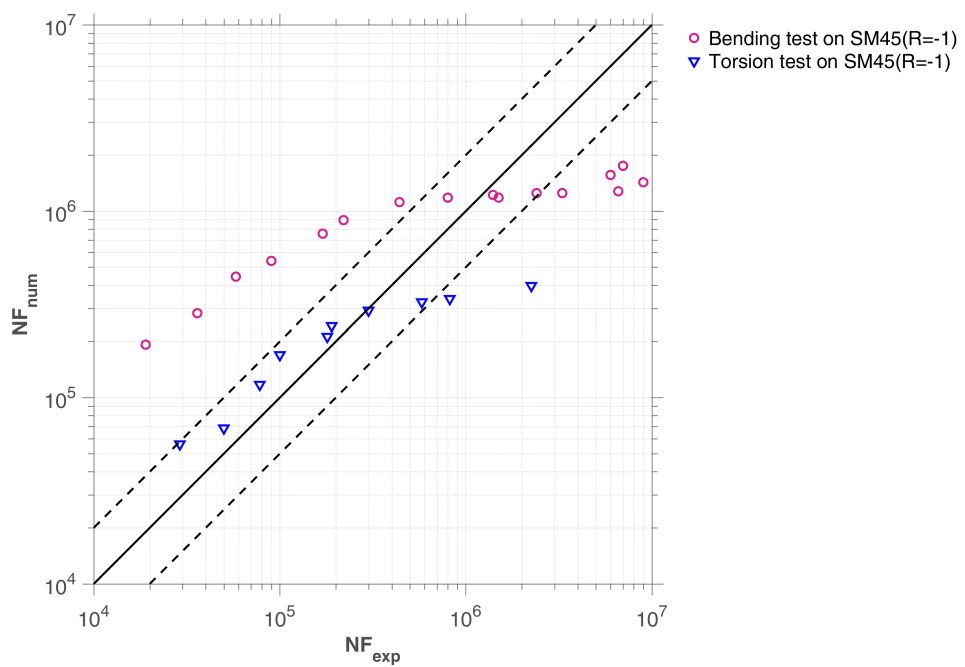
Although the uniaxial experimental data we extracted from Lee's curve [8] of SM45C steel are slightly dispersed, we can find our model quite satisfactory in the case of SM45C steel. As for multiaxial 90 degree out of phase, fully reversed bending-torsion fatigue tests, our model is able to evaluate the cycles to failure.

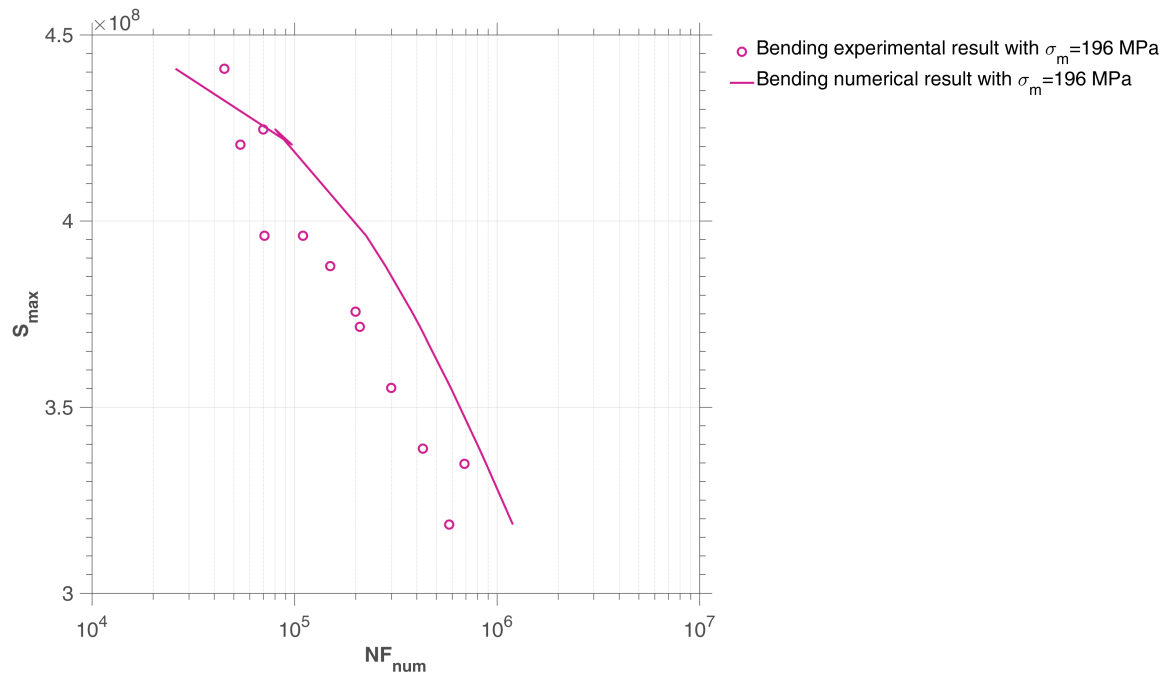
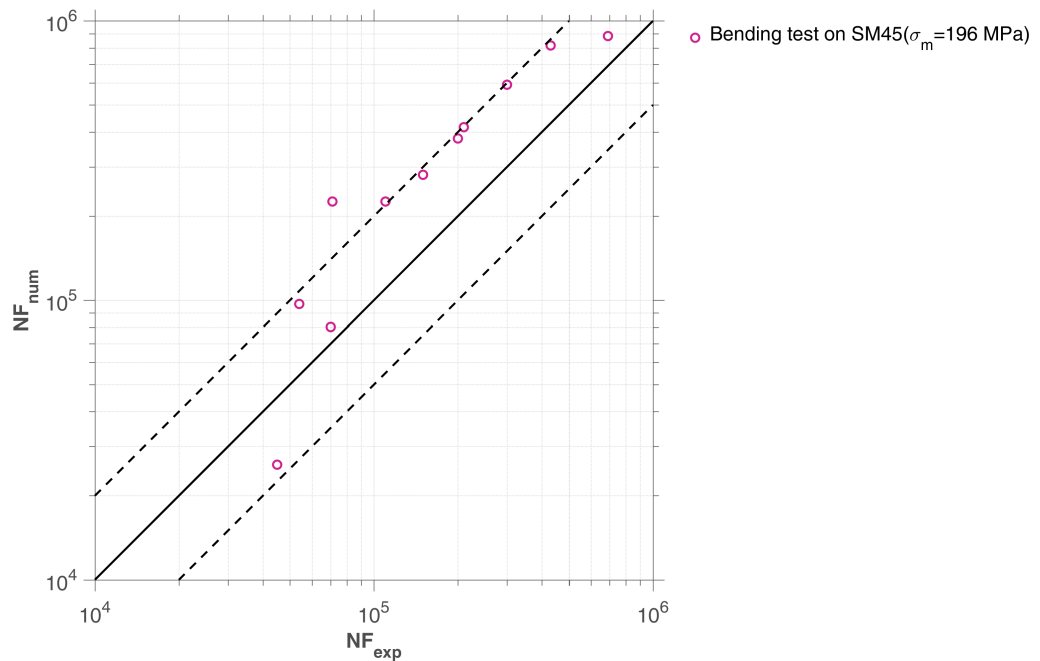
Group	N [Cycles]	τ_a [MPa]	σ_a [MPa]	σ_m [MPa]
A	29.9E3	282	449	0
	35.7E3	334	354	0
	50E3	223	485	0
	73.8E3	309	357	0
	106E3	217	449	0
	106E3	285	370	0
	112E3	199	449	0
	131E3	194	457	0
	333E3	252	354	0
B	431E3	154	437	0
	53E3	215	441	196
	59.2E3	309	286	196
	70.1E3	155	464	196
	86.3E3	136	473	196
	89.9E3	334	173	196
	92.1E3	209	403	196
	102E3	177	437	196
	135E3	321	167	196
	351E3	179	357	196
	394E3	274	182	196

Table 20: With and without mean bending stress on out-of-phase(90°) fatigue of SM45C steel [8]

β	λ	W_0/a
3.8	0.55	1000 GPa

Table 21: Parameter identification of 30NCD16 steel

Figure 32: Bending and torsion test on SM45C steel($R=-1$)Figure 33: Bending and torsion test on SM45C steel($R=-1$)

Figure 34: Bending test with mean stress on SM45C steel($R=-1, \sigma_m = 196 \text{ MPa}$)Figure 35: Bending test with mean stress on SM45C steel($R=-1, \sigma_m = 196 \text{ MPa}$)

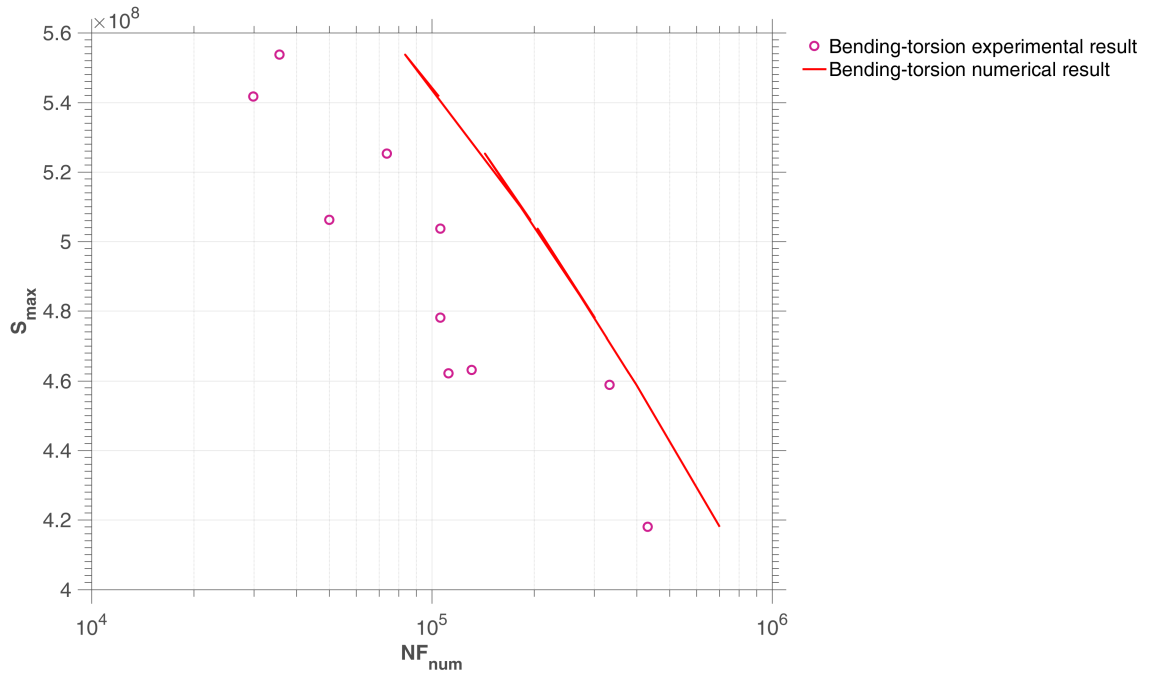


Figure 36: Calibrated S-N curve of SM45C steel under fully reversed bending-torsion tests

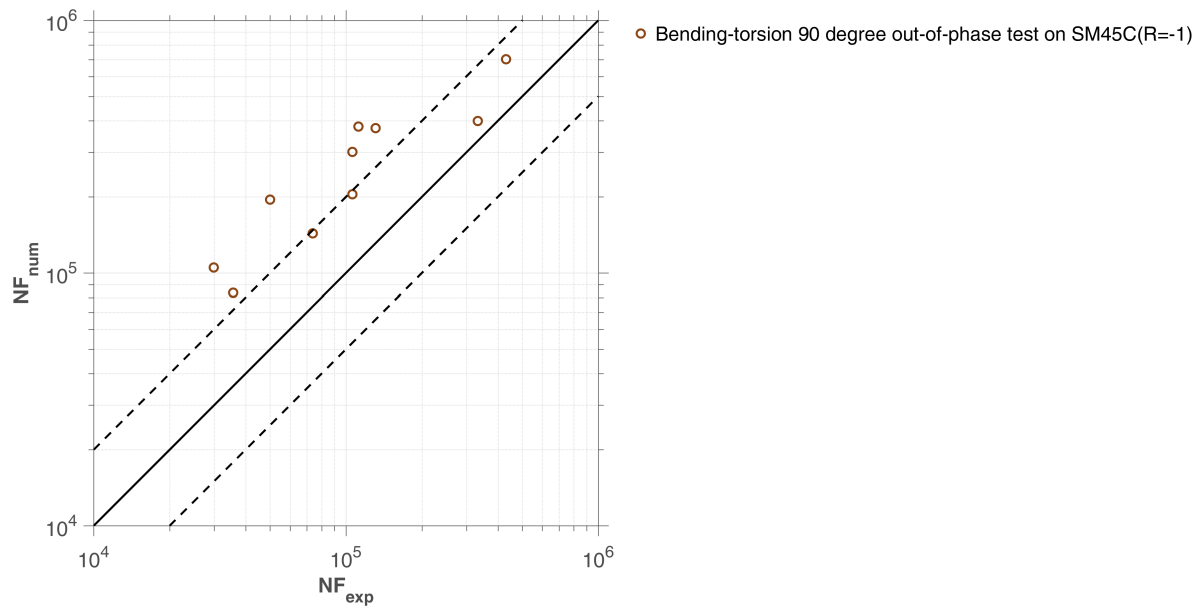


Figure 37: Calibrated S-N curve of SM45C steel under fully reversed bending-torsion tests

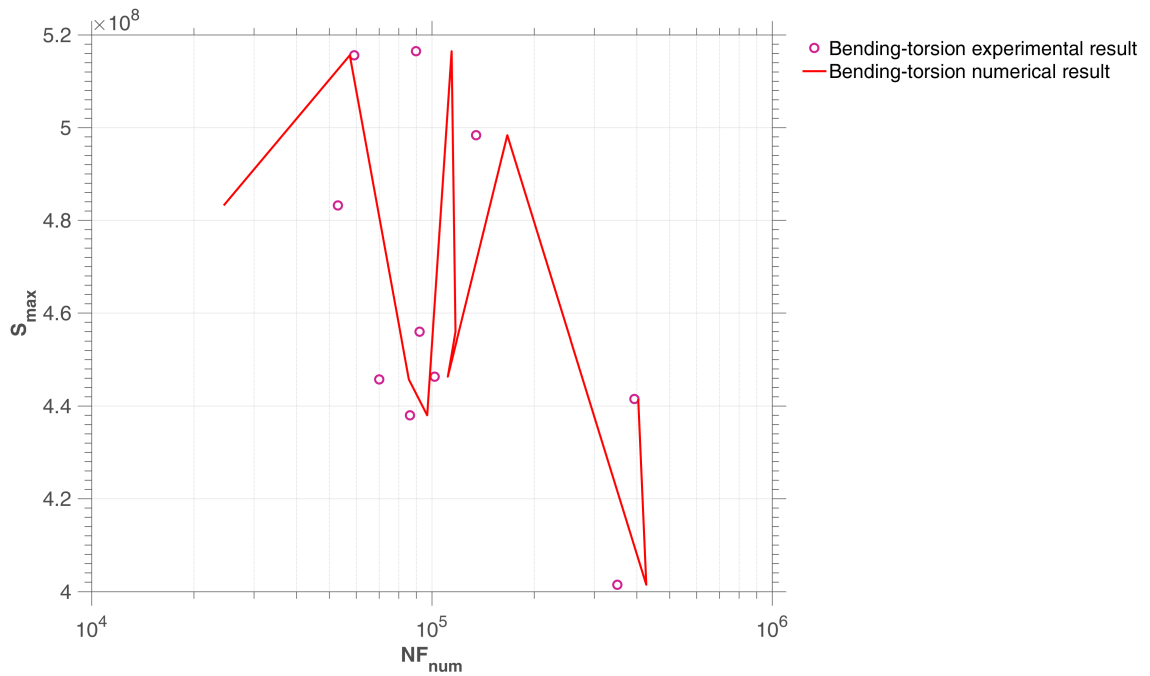


Figure 38: Calibrated S-N curve of SM45C steel under fully reversed bending-torsion tests with mean stress

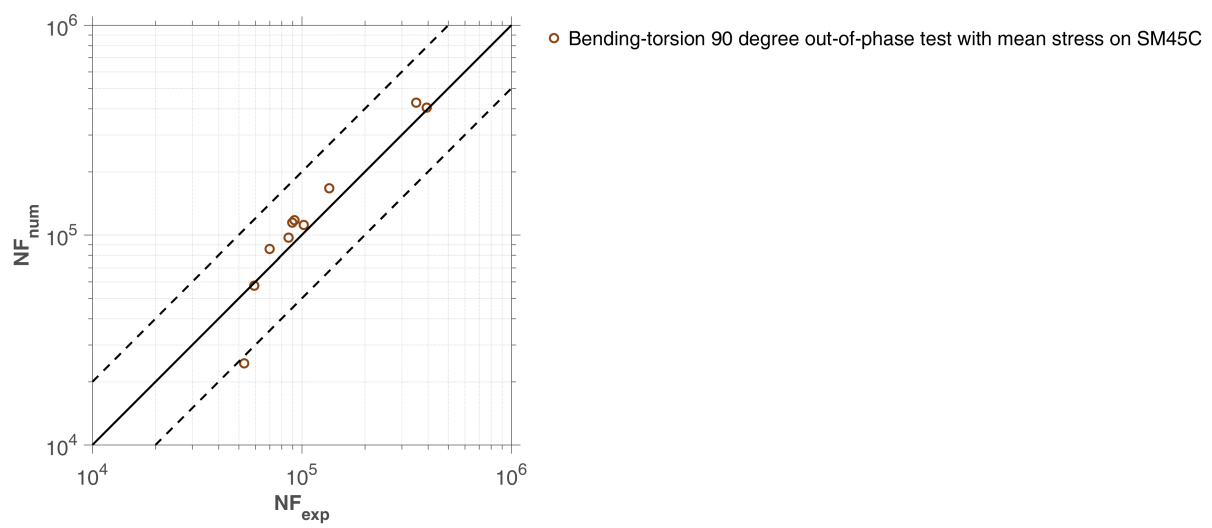


Figure 39: Calibrated S-N curve of SM45C steel under fully reversed bending-torsion tests with mean stress

6.5. Experimental validation of the model on 10 HNAP steel

6.5.1. Presentation of the material

Fatigue tests were performed on the HNAP steel. It is a very low carbon steel which resembles the 10 CN 6. In Table.22, its chemical composition is given: The mechanical properties of this steel are given in

C	Mn	Si	P	S	Cr	Cu	Ni	Fe
0.12%	0.71%	0.41%	0.08%	0.03%	0.81%	0.30%	0.50%	the rest

Table 22: Chemical composition of 10 HNAP steel[9]

Table.23:

$Re_{0.2\%}$	R_m	A	ν	E
418 MPa	566 Mpa	32%	0.29	215000 Mpa

Table 23: Mechanical characteristics of steel 10 HNAP[?]

where

- Σ_e : elastic limit at 0.2% of plastic deformation,
- R_m : maximum tensile strength,
- A : elongation at break,
- ν : Poisson's coefficient,
- E : Young's modulus.

6.5.2. Description of fatigue tests on 10 HNAP steel

The Macha team performed a large number of fatigue tests on the HNAP steel. Thus, it performed not only simple tensile compression and torsion tests ($R = -1$) in order to establish The corresponding Wöhler curves but also tests under variable loading on cylindrical specimens of the same material[10]. VIDAL[11] carried out tensile tests on this material for various mean stress values. It has established the Wöhler curve in repeated traction in order to validate on this steel the method of Robert whose use requires three Wöhler curves in symmetrical alternating traction, symmetrical alternating torsion and repetitive traction.

Wöhler curve in tension-compression

The model chosen by Macha and recovered by Jabbado[12] for the tensile-compression Wöhler curve is that of Basquin:

$$\ln N = 68.361 - 9.82 \ln (\sigma_{-1}) \quad (52)$$

56

Wöhler curve in symmetrical alternating torsion

The symmetric alternating torsion Wöhler curve was recovered by Jabbado[12] using following equation:

$$\ln N = 21.55 - 0.0385\tau_{-1} \quad (53)$$

Tensile fatigue tests for various mean stress values

VIDAL[11] carried out tensile tests on HNAP steel for various values of mean stress. The results are summarized in Table.24. They allowed us to plot the Wöhler curves for different values of the mean stress σ_m . These curves are modeled by the Wöhler equation:

$$\ln N = A - B\sigma_{max} \quad (54)$$

In the Table.??, the values of the constants A and B of Eq.(54).

σ_a (MPa)	σ_m (MPa)	N_{exp} (cycles)
250	75	439300;402500
270	75	358200;854700;318700
290	75	252300;376300;379700
310	75	54800;123400;45000
250	150	157400;1333000
270	150	172100;121500;233100
290	150	124300;41900;60500
230	225	413900;204500;545200
250	225	122400;229600;104000
270	225	110000;29900;66000
190	300	497100;234300;524800
210	300	463500;367300;259500
230	300	219000;179400;222400
250	300	95300;118200;59100

Table 24: Experimental results of tensile tests for various values of σ_m

Fatigue testing under variable loading

Random multiaxial loading fatigue tests were performed on cylindrical HNAP steel specimens[10]. The load considered is proportional and results from a combination of bending and torsion. The random signal is stationary and has a normal distribution as a probability distribution. Tests of this type have been analyzed and simulated by Carpinteri et al.[13]. They were provided to us in the form of tests carried out on the HNAP steel for two values of the angle α' : $\alpha' = \pi/8$ and $\alpha' = \pi/4$. α' is the angle made by the resultant moment M with the bending moment M_B (see Figure 40).

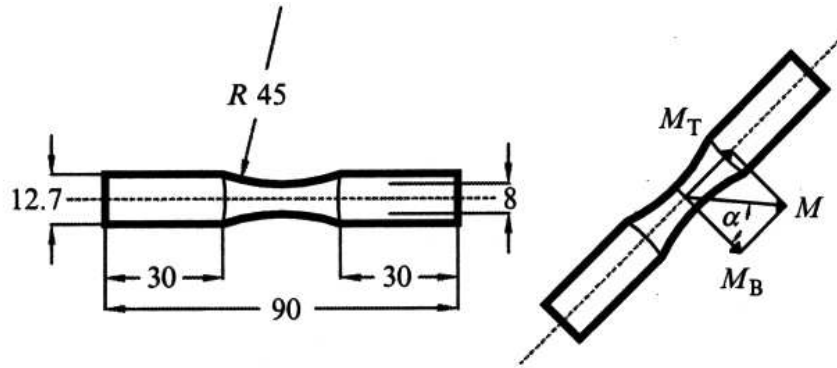


Figure 40: Bending-torsion fatigue tests on cylindrical specimens[13]

The stationary random loading sequence contains 49152 values recorded by a time interval of 0.00375 seconds (frequency = 266.67 Hz). It is shown in Figure 41. Its total duration is 184.32 seconds. This sequence is multiplied by load coefficients corresponding to bending $f(\sigma_{xx})$ and torsion $f(\tau_{xy})$ in order to obtain random multiaxial loading sequences. As the signal is stationary, the breaking life is determined in terms of number of sequences with break N_{Sq} . Knowing N_{Sq} and the total time in seconds of the sequence studied, it is easy to express the lifetime of the piece in seconds. The results of fatigue tests under variable loads are summarized in Table.25 and Table.26 as a function of angle α' and ratio r ; $r = f(\tau_{xy})/f(\sigma_{xx})$.

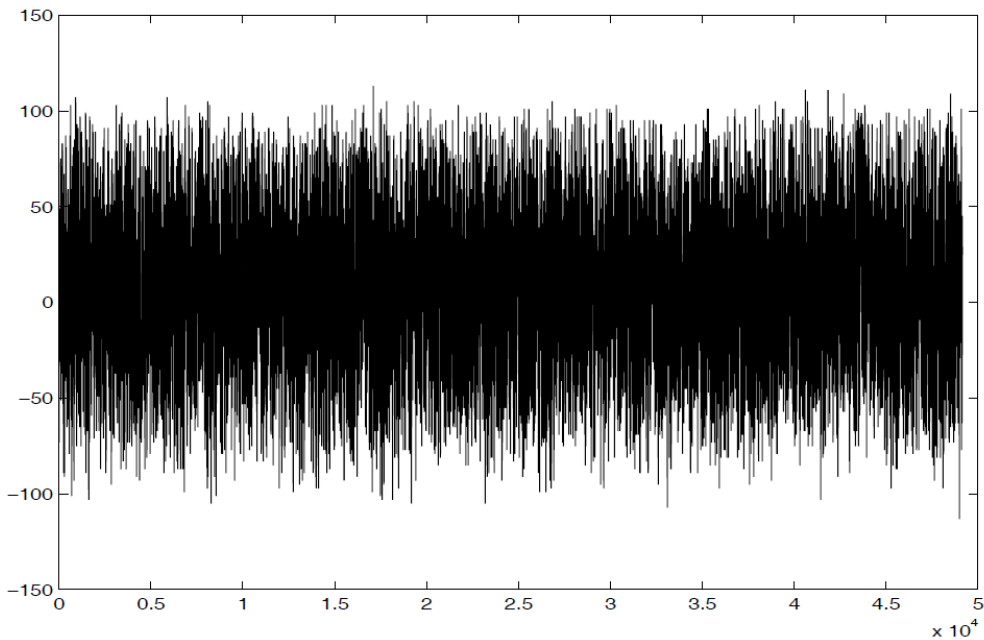


Figure 41: Bending-torsion fatigue tests on cylindrical specimens[13]

1st type of tests: $\alpha' = \pi/8$ and $r = f(\tau_{xy})/f(\sigma_{xx}) = 0.2$.

N^o	$f(\sigma_{xx})$	$f(\tau_{xy})$	r	$T_{exp}(s)$
1	5.7084	1.1822	0.2	16843.2
2	5.2917	1.0959	0.2	17780.1
3	4.8337	1.0010	0.2	24416.5
4	5.2674	1.0909	0.2	24858.2
5	5.4534	1.1294	0.2	26518.3
6	5.2002	1.0769	0.2	36162.3
7	4.7944	0.9929	0.2	47600.4
8	4.3862	0.9084	0.2	57993.9
9	4.6241	0.9576	0.2	60428
10	4.0194	0.8324	0.2	73373.3
11	4.0127	0.8310	0.2	87609.1
12	4.2292	0.8758	0.2	89185.2
13	3.9213	0.8121	0.2	106900
14	3.7731	0.7814	0.2	117358
15	4.1148	0.8521	0.2	118902
16	3.6150	0.7486	0.2	132448
17	3.3135	0.6862	0.2	170571
18	4.1298	0.8553	0.2	178215
19	3.4761	0.7199	0.2	225288
20	3.3430	0.6923	0.2	352635
21	3.0135	0.6241	0.2	355720

Table 25: Fatigue results under variable loads for $\alpha' = \pi/8$ and $r = f(\tau_{xy})/f(\sigma_{xx}) = 0.2$

2nd type of tests: $\alpha' = \pi/4$ and $r = f(\tau_{xy})/f(\sigma_{xx}) = 0.5$.

In Figure 42, an example of a random multiaxial loading sequence is given.

6.5.3. Identification of model parameters of 10HNAP steel

As mentioned earlier, the identification of the model parameters requires a Wöhler curve. This initiates the value of β , in the mean stress tests we have got the value of λ . And the value of W_0 and a comes from random loading. The parameters of the HNAP steel model can be identified by referring to Table 27. They are grouped in the following table:

N^o	$f(\sigma_{xx})$	$f(\tau_{xy})$	r	$T_{exp}(s)$
1	4.2519	2.126	0.5	15379.4
2	4.0567	2.0284	0.5	21465.7
3	3.8982	1.9491	0.5	25350.4
4	3.7823	1.8912	0.5	45949
5	3.5963	1.7982	0.5	62434.8
6	3.4497	1.7249	0.5	75225.7
7	2.9423	1.4712	0.5	115009
8	2.8814	1.4407	0.5	136794
9	2.3299	1.165	0.5	203365
10	2.8399	1.42	0.5	221370
11	2.8493	1.4247	0.5	244757
12	2.2542	1.1271	0.5	251723
13	2.3651	1.1826	0.5	288080
14	2.4215	1.2108	0.5	405444

Table 26: Fatigue results under variable loads for $\alpha' = \pi/4$ and $r = f(\tau_{xy})/f(\sigma_{xx}) = 0.5$

β	λ	W_0/a
1.85	0.85	440e9

Table 27: Model parameters for 10HNAP steel

6.5.4. Simulation of fatigue tests performed on 10HNAP steel

After determining the parameters of the HNAP steel model and calculated pc_s for each of the tests tested, the number of priming cycles can be obtained by directly applying equation (2.87) for the proportional periodic loads of Constant amplitude and By applying equation (2.89) for multiaxial loadings of variable amplitude.

In Figure 43 and Figure 44, we give the prediction results of the tensile-compression tests used to identify the parameters of the model, as well as those in purely alternating torsion. These are to be taken with caution because of the effect of the gradient because the specimens stressed in tension and in torsion are not of the same nature.

The tensile Wöhler curves for various values of the mean stress are given in Figure 45.

The prediction results of the tensile tests for various values of the mean stress m are summarized in Figure 46. These results correlate well with the experimental lifetimes. The tests of multiaxial loadings of variable amplitude are plotted in Figures (3.27) and (3.28) as a function of the angle α' and the ratio r . In

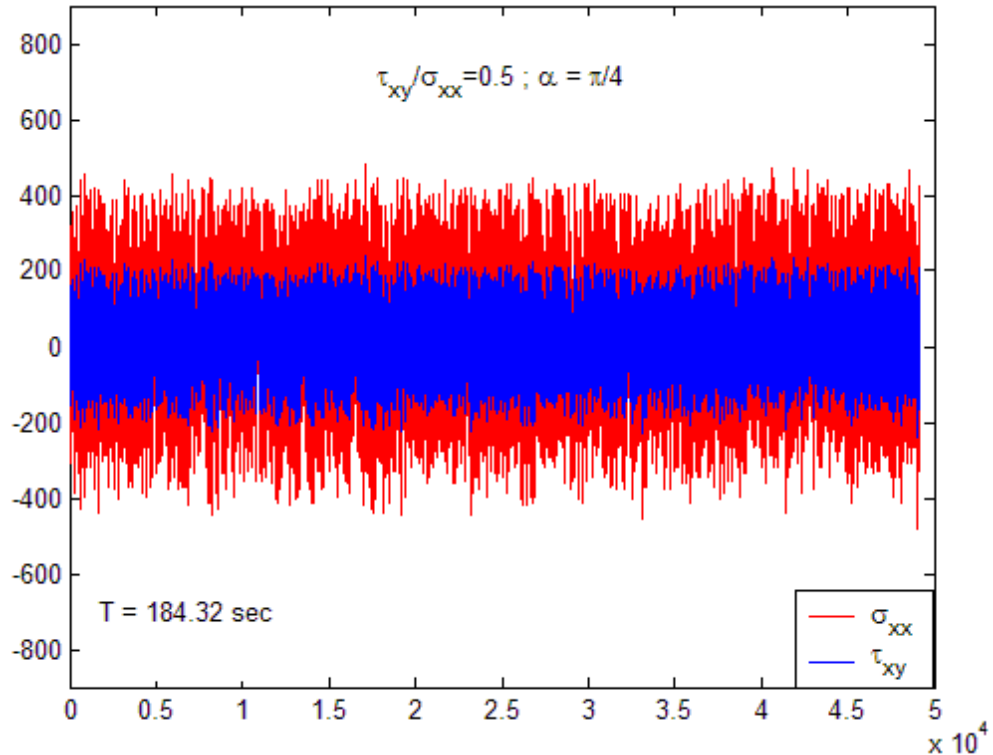
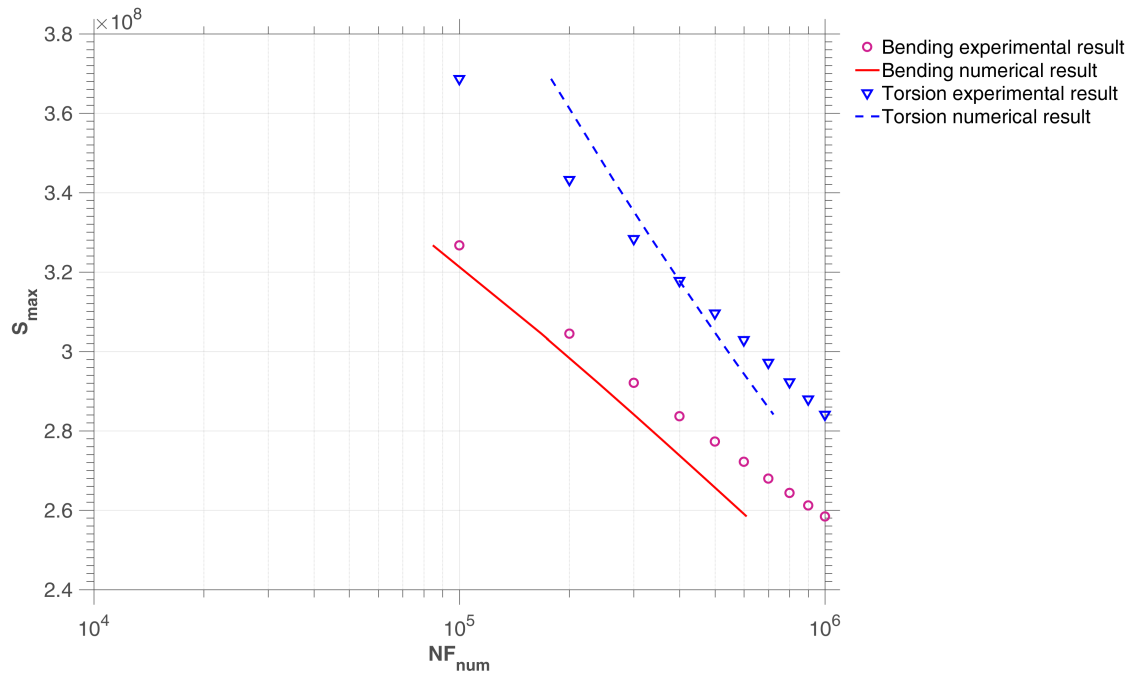
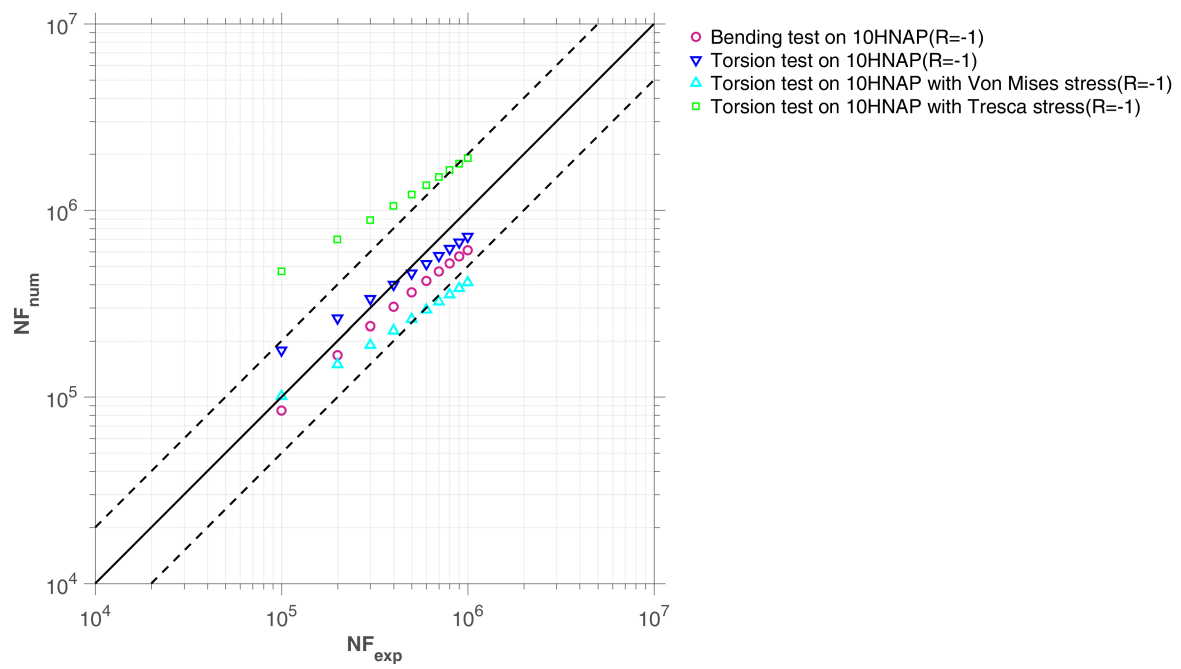


Figure 42: Multiaxial random loading sequence

these figures, the prediction results of the proposed model and that presented by Carpinteri et al. [17]. For the first type of tests ($\sigma_{xx} = \tau_{xy} = 8$ and $r = 0.2$), the best predictions are given by the proposed model. However, for the second type of tests ($\sigma_{xx} = \tau_{xy} = 4$ and $r = 0.5$), the predictions of Carpinteri et al. [17] are relatively better.

FIG. 3.27

FIG. 3.28

Figure 43: Bending and torsion test on 10HNAP steel($R=-1$)Figure 44: Bending and torsion test on 10HNAP steel($R=-1$)

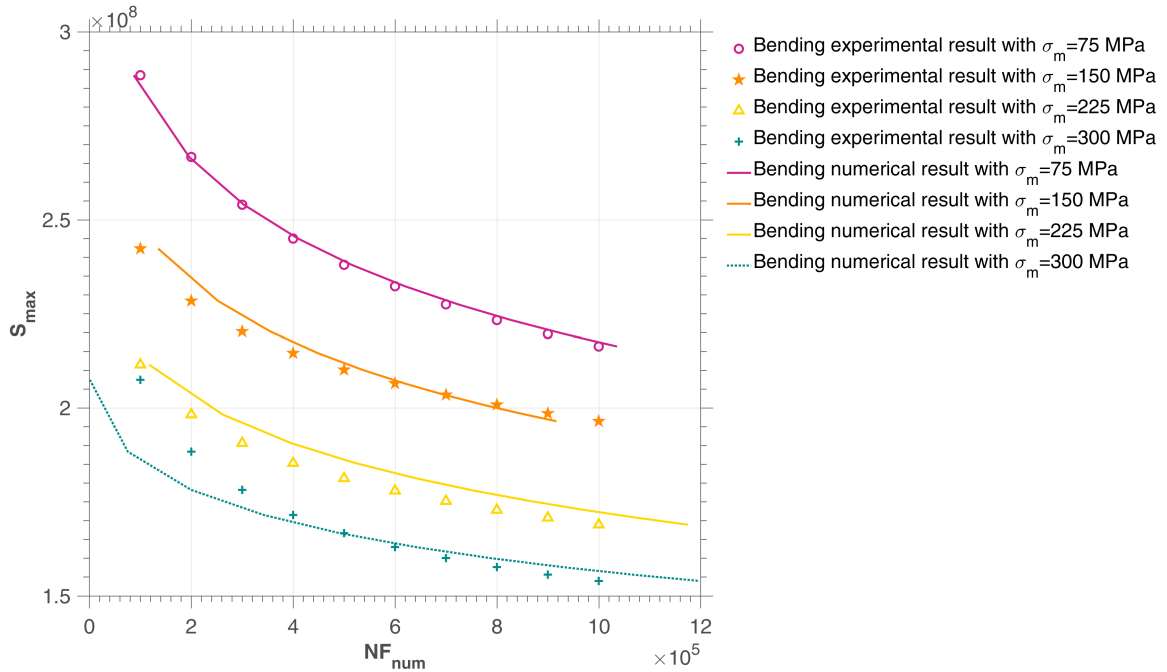


Figure 45: Wöhler tensile curves for various mean stress values

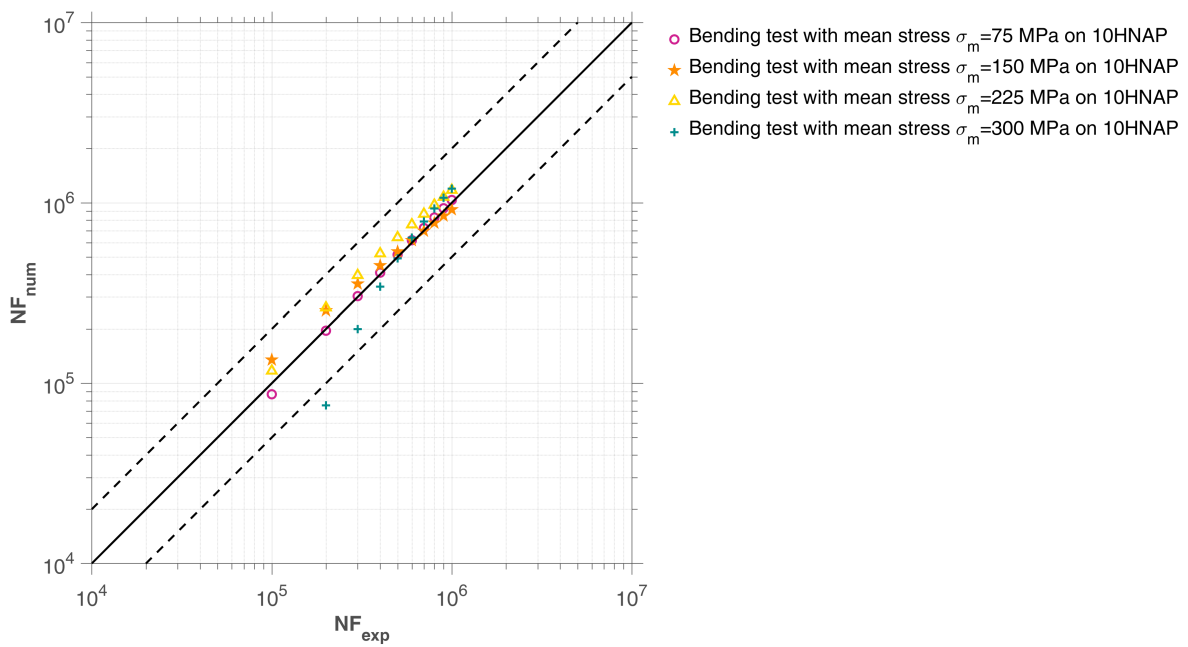


Figure 46: Wöhler tensile curves for various mean stress values

7 Discussion

We work on the stress tensor directly in 3D analysis in stead of using the multidimensional equivalent stress. The strategy can be made more complex by introducing a local space averaging process in the calculation of the local damage, and by taking more general plastic flows. The energy based fatigue approach takes into account impurities and hardness in the material and is applicable to any type of micro plasticity law and multiaxial load geometry. The time implicit strategy gets rid of cycle counting which is hardly applicable to complex loading, big fluctuation is magnified which reflects the real situation.

The advantages and drawbacks of our proposed model are listed as follows:

1. No rain-flow filter
2. No cycle counting
3. Possible handling of different SN curves.
4. Random loading suitability with nonlinear damage accumulation
5. Requires a scale by scale analysis
6. Real multi-axial tests to be applied.

Acknowledgments

We are grateful for the financial and technical support of Chaire PSA.

References

- [1] M. Maitournam, C. Krebs, A. Galtier, [A multiscale fatigue life model for complex cyclic multiaxial loading](#), International Journal of Fatigue 33 (2) (2011) 232 – 240. [doi:
http://dx.doi.org/10.1016/j.ijfatigue.2010.08.017](http://dx.doi.org/10.1016/j.ijfatigue.2010.08.017).
URL <http://www.sciencedirect.com/science/article/pii/S0142112310001933>
- [2] S. Bosia, A. Constantinescu, [Fast time-scale average for a mesoscopic high cycle fatigue criterion](#), International Journal of Fatigue 45 (2012) 39 – 47. [doi:
http://dx.doi.org/10.1016/j.ijfatigue.2012.06.015](http://dx.doi.org/10.1016/j.ijfatigue.2012.06.015).
URL <http://www.sciencedirect.com/science/article/pii/S0142112312002162>
- [3] M. Zepeng, Structures under multiaxial fatigue taking consideration of gradients of the constraints with time and space variation.
- [4] J. Lemaitre, J.-L. Chaboche, Mechanics of solid materials, Cambridge university press, 1990.
- [5] Legendre Gauss Quadrature weights and nodes, <https://www.mathworks.com/matlabcentral/fileexchange/4540-legendre-gauss-quadrature-weights-and-nodes>, accessed: 2004-05-11.
- [6] G. DIETER, MECHANICAL METALLURGY, 1961.
- [7] L. DUBAR, Fatigue multiaxiale des aciers - passage de l'endurance à l'endurance limitée -prise en compte des accidents géométriques., Thèse de Doctorat,Ecole Nationale Supérieure d'Arts et Métiers, Talence, France.
- [8] S.-B. Lee, Out-of-phase combined bending and torsion fatigue of steels, ICBMFF2.

- [9] W. Bedkowski, Determination of the critical plane and effort criterion in fatigue life evaluation for materials under multiaxial random loading. experimental verification based on fatigue tests of cruciform specimens (1994) s.435–447.
- [10] B. W. G. J. M. E. ACHTELIC, H., Fatigue life of 10hnap steel under synchronous random bending and torsion. (1994) 421–434.
- [11] E. VIDAL, Prévision de la durée de vie en fatigue multiaxiale sous sollicitations d'amplitude variable à l'aide d'un critère global.
- [12] M. Jabbado, *High-Cycle Fatigue of Metallic Structures : Lifetime Duration under Variable Loadings.*, Theses, Ecole Polytechnique X (Mar. 2006).
URL <https://pastel.archives-ouvertes.fr/pastel-00002116>
- [13] A. Carpinteri, A. Spagnoli, S. Vantadori, A multiaxial fatigue criterion for random loading, *Fatigue & Fracture of Engineering Materials & Structures* 26 (6) (2003) 515–522.

Appendices

Appendix A DETAILED EXPLOITATION

A DETAILED DESCRIPTION OF ANALYTICAL EXPLOITATION ON UNIAXIAL CYCLE

Phase 1: The deviatoric stress amplitude increases from σ_y/s to S_{max} .

The material is in local plastic regime, then $\dot{\varepsilon}^p > 0$ and $\dot{\sigma} - \dot{b} = 0 \Rightarrow \dot{\Sigma} - \frac{E}{1+\nu} \dot{\varepsilon}^p = \frac{kE}{E-k} \dot{\varepsilon}^p \Rightarrow$

$$\dot{\varepsilon}^p = \frac{(E-k)(1+\nu)}{E(E+k\nu)} \dot{\Sigma}.$$

$\Rightarrow \dot{\varepsilon}^p$ varies from 0 to $\frac{(E-k)(1+\nu)(S_{max} - \sigma_y/s)}{E(E+k\nu)}$.

From Taylor-Lin scale transition model:

$$\dot{\sigma} = \dot{\Sigma} - \frac{E}{1+\nu} \dot{\varepsilon}_p = \dot{\Sigma} - \frac{E-k}{E-\nu k} \dot{\Sigma} = \frac{k(1-\nu)}{E-k\nu} \dot{\Sigma}.$$

$\Rightarrow \sigma$ varies from σ_y/s to $\sigma_y/s + \frac{k(1-\nu)(S_{max} - \sigma_y/s)}{E-k\nu}$.

$$\dot{b} = \dot{\Sigma} - \frac{E}{1+\nu} \dot{\varepsilon}_p = \dot{\Sigma} - \frac{E-k}{E-\nu k} \dot{\Sigma} = \frac{k(1-\nu)}{E-k\nu} \dot{\Sigma}.$$

$\Rightarrow b$ varies from 0 to $\frac{k(1-\nu)(S_{max} - \sigma_y/s)}{E-k\nu}$.

So the energy dissipation rate is:

$$(\sigma - b) \dot{\varepsilon}^p = \frac{\sigma_y}{s} \dot{\varepsilon}^p = \frac{\sigma_y}{s} \frac{(E-k)(1+\nu)}{E(E+k\nu)} \dot{\Sigma}.$$

The energy dissipation is:

$$(\sigma - b) \Delta \varepsilon^p = \frac{\sigma_y}{s} \frac{(E-k)(1+\nu)(S_{max} - \sigma_y/s)}{E(E+k\nu)}.$$

Phase 2: The deviatoric stress amplitude decreases from S_{max} to $S_{max} - 2\sigma_y/s$.

The material is in local elastic regime, then $\dot{\varepsilon}^p = 0$ and $\dot{\sigma} - \dot{b} = 0 \Rightarrow$

$$\dot{b} = 0, \dot{\sigma} = \dot{\Sigma} - \frac{E}{1+\nu} \dot{\varepsilon}_p = \dot{\Sigma}.$$

σ varies from $\sigma_y/s + \frac{k(1-\nu)(S_{max} - \sigma_y/s)}{E-k\nu}$ to $-\sigma_y/s + \frac{k(1-\nu)(S_{max} - \sigma_y/s)}{E-k\nu}$.

$\sigma - b$ varies from σ_y/s to $-\sigma_y/s$.

The energy dissipation rate is:

$$(\sigma - b)\dot{\varepsilon}^p = 0.$$

Phase 3: The deviatoric stress amplitude decreases from $S_{max} - 2\sigma_y/s$ to $-S_{max}$.

The material is in local plastic regime, then $\dot{\varepsilon}^p > 0$ and $\dot{\sigma} - \dot{b} = 0 \Rightarrow$

$$\dot{\varepsilon}^p = \frac{(E - k)(1 + \nu)}{E(E + k\nu)} \dot{\Sigma}$$

as opposite to phase 1 for $\dot{\Sigma} < 0$.

$$\Rightarrow \dot{\varepsilon}^p \text{ varies from } \frac{(E - k)(1 + \nu)(S_{max} - \sigma_y/s)}{E(E + k\nu)} \text{ to } \frac{(E - k)(1 + \nu)(S_{max} - \sigma_y/s - S_{max} - (S_{max} - 2\sigma_y/s))}{E(E + k\nu)} = -\frac{(E - k)(1 + \nu)(S_{max} - \sigma_y/s)}{E(E + k\nu)}.$$

From Taylor-Lin scale transition model:

$$\dot{\sigma} = \dot{\Sigma} - \frac{E}{1 + \nu} \dot{\varepsilon}_p = \dot{\Sigma} - \frac{E - k}{E - \nu k} \dot{\Sigma} = \frac{k(1 - \nu)}{E - \nu k} \dot{\Sigma}.$$

$$\Rightarrow \sigma \text{ varies from } -\sigma_y/s + \frac{k(1 - \nu)(S_{max} - \sigma_y/s)}{E - \nu k} \text{ to } -\sigma_y/s - \frac{k(1 - \nu)(S_{max} - \sigma_y/s)}{E - \nu k}.$$

$$\dot{b} = \dot{\Sigma} - \frac{E}{1 + \nu} \dot{\varepsilon}_p = \dot{\Sigma} - \frac{E - k}{E - \nu k} \dot{\Sigma} = \frac{k(1 - \nu)}{E - \nu k} \dot{\Sigma}.$$

$$\Rightarrow b \text{ varies from } \frac{k(1 - \nu)(S_{max} - \sigma_y/s)}{E - \nu k} \text{ to } -\frac{k(1 - \nu)(S_{max} - \sigma_y/s)}{E - \nu k}.$$

So the energy dissipation rate is:

$$(\sigma - b)\dot{\varepsilon}^p = -\frac{\sigma_y}{s} \dot{\varepsilon}^p = -\frac{\sigma_y}{s} \frac{(E - k)(1 + \nu)}{E(E + k\nu)} \dot{\Sigma}.$$

The energy dissipation is:

$$(\sigma - b)\Delta\varepsilon^p = -\frac{\sigma_y}{s} \frac{(E - k)(1 + \nu)(-2S_{max} + 2\sigma_y/s)}{E(E + k\nu)} = \frac{2\sigma_y}{s} \frac{(E - k)(1 + \nu)(S_{max} - \sigma_y/s)}{E(E + k\nu)}.$$

Phase 4: The deviatoric stress amplitude increases from $-S_{max}$ to $-S_{max} + 2\sigma_y/s$.

The material is in local elastic regime, then $\dot{\varepsilon}^p = 0$ and $\dot{\sigma} - \dot{b} = 0 \Rightarrow$

$$\dot{b} = 0, \dot{\sigma} = \dot{\Sigma} - \frac{E}{1 + \nu} \dot{\varepsilon}_p = \dot{\Sigma}.$$

$$\sigma \text{ varies from } -\sigma_y/s - \frac{k(1 - \nu)(S_{max} - \sigma_y/s)}{E - \nu k} \text{ to } \sigma_y/s - \frac{k(1 - \nu)(S_{max} - \sigma_y/s)}{E - \nu k}.$$

$\sigma - b$ varies from $-\sigma_y/s$ to σ_y/s .

So the energy dissipation rate is:

$$(\sigma - b)\dot{\varepsilon}^p = 0.$$

Phase 5: The deviatoric stress amplitude increases from $-S_{max} + 2\sigma_y/s$ to σ_y/s .

The material is in local plastic regime, then $\dot{\varepsilon}^p > 0$ and $\dot{\sigma} - \dot{b} = 0 \Rightarrow$

$$\dot{\varepsilon}^p = \frac{(E - k)(1 + \nu)}{E(E + k\nu)} \dot{\Sigma}$$

as in phase 1.

$$\Rightarrow \dot{\varepsilon}^p \text{ varies from } -\frac{(E - k)(1 + \nu)(S_{max} - \sigma_y/s)}{E(E + k\nu)} \text{ to } 0.$$

$$\dot{\sigma} = \dot{\Sigma} - \frac{E}{1 + \nu} \dot{\varepsilon}^p = \dot{\Sigma} - \frac{E - k}{E - \nu k} \dot{\Sigma} = \frac{k(1 - \nu)}{E - k\nu} \dot{\Sigma}.$$

$$\Rightarrow \sigma \text{ varies from } \sigma_y/s - \frac{k(1 - \nu)(S_{max} - \sigma_y/s)}{E - k\nu} \text{ to } \sigma_y/s.$$

$$\dot{b} = \dot{\Sigma} - \frac{E}{1 + \nu} \dot{\varepsilon}^p = \dot{\Sigma} - \frac{E - k}{E - \nu k} \dot{\Sigma} = \frac{k(1 - \nu)}{E - k\nu} \dot{\Sigma}.$$

$$\Rightarrow b \text{ varies from } -\frac{k(1 - \nu)(S_{max} - \sigma_y/s)}{E - k\nu} \text{ to } 0.$$

So the energy dissipation rate is:

$$(\sigma - b) \dot{\varepsilon}^p = \frac{\sigma_y}{s} \dot{\varepsilon}^p = \frac{\sigma_y}{s} \frac{(E - k)(1 + \nu)}{E(E + k\nu)} \dot{\Sigma}.$$

The energy dissipation is:

$$(\sigma - b) \Delta \varepsilon^p = \frac{\sigma_y}{s} \frac{(E - k)(1 + \nu)(S_{max} - \sigma_y/s)}{E(E + k\nu)}.$$

From the three phase analysis in local plastic regime, the dissipated energy is like $dW(\text{phase1}) = \frac{1}{2} dW(\text{phase3}) = dW(\text{phase5})$ and the dissipation rate is like $d\dot{W}(\text{phase1}) = d\dot{W}(\text{phase3}) = d\dot{W}(\text{phase5})$.

$$d\dot{W} = \frac{(E - k)(1 + \nu)}{E(E - k\nu)} \left(\frac{\sigma_y}{s} \right) |\dot{\Sigma}| \quad (\text{A.1})$$

MULTI-DIMENSIONAL PLASTIC AND ELASTIC REGIME ANALYSIS

At a certain scale s_i , after elimination of $\underline{\dot{\epsilon}}^p$, there are

$$\underline{\dot{S}} - \underline{\dot{b}} = dev \underline{\dot{\Sigma}} - E\gamma \left(\frac{1}{1+\nu} + \frac{k}{E-k} \right) \frac{\underline{S} - \underline{b}}{\|\underline{S} - \underline{b}\|}.$$

If we are at yield limit at $(t+dt)$, we get on the other hand:

$$\begin{aligned} \left(\underline{S} - \underline{b} \right) (t+dt) &= \left(\underline{S} - \underline{b} \right) (t) + \left(\dot{\underline{S}} - \dot{\underline{b}} \right) dt, \\ \left\| \left(\underline{S} - \underline{b} \right) (t+dt) \right\| &= (\sigma_y - \lambda\sigma_m) / s_i. \end{aligned} \quad (\text{A.2})$$

Replacing $\left(\dot{\underline{S}} - \dot{\underline{b}} \right)$ in the integration by its expression we get:

$$\left(\underline{S} - \underline{b} \right) (t+dt) = \left(\underline{S} - \underline{b} \right) (t) + dev \underline{\dot{\Sigma}} dt - E\gamma dt \left(\frac{1}{1+\nu} + \frac{k}{E-k} \right) \frac{\left(\underline{S} - \underline{b} \right) (t+dt)}{\|\underline{S} - \underline{b}\| (t+dt)} \quad (\text{A.3})$$

Putting all terms with $\left(\underline{S} - \underline{b} \right) (t+dt)$ on the left hand side, we get:

$$\left(\underline{S} - \underline{b} \right) (t+dt) (1+\eta) = \left(\underline{S} - \underline{b} \right) (t) + dev \underline{\dot{\Sigma}} dt = \left(\underline{S} - \underline{b} \right)_{trial} (t+dt) \quad (\text{A.4})$$

with

$$\eta = \frac{E\gamma dt}{\|\underline{S} - \underline{b}\| (t+dt)} \left(\frac{1}{1+\nu} + \frac{k}{E-k} \right). \quad (\text{A.5})$$

To see whether the structure is in elastic or plastic regime at each time step, we use $\left(\underline{S} - \underline{b} \right)_{trial} (t+dt)$ to compare with the yield stress at the same scale s_i , thus to give a value to $\left(\underline{S} - \underline{b} \right) (t+dt)$.

Since $\left(\underline{S} - \underline{b} \right) (t+dt)$ is in the same direction as $\left(\underline{S} - \underline{b} \right)_{trial} (t+dt)$, we have

$$\left(\underline{S} - \underline{b} \right) (t+dt) = (\sigma_y - \lambda\sigma_H(t+dt)) / s \frac{\left(\underline{S} - \underline{b} \right)_{trial} (t+dt)}{\|\underline{S} - \underline{b}\|_{trial} (t+dt)} \quad (\text{A.6})$$

We now compare Eq.(A.4) and Eq.(A.6), the only solution is to have:

$$1 + \eta = \frac{\|\underline{S} - \underline{b}\|_{trial}}{(\sigma_y - \lambda\sigma_m) / s} \quad (\text{A.7})$$

that is:

$$\eta = \frac{\|\underline{S} - \underline{b}\|_{trial}}{(\sigma_y - \lambda\sigma_m) / s} - 1 \quad (\text{A.8})$$

which is positive in plastic regime.